JYVÄSKYLÄ STUDIES IN COMPUTING 47

Viatcheslav Solbakov

Application of Mathematical Modeling for Water Environment Problems

Esitetään Jyväskylän yliopiston informaatioteknologian tiedekunnan suostumuksella
julkisesti tarkastettavaksi Villa Rana-rakennuksen Paulaharju -salissa
joulukuun 22. päivänä 2004 kello 12.

Academic dissertation to be publicly discussed, by permission of
the the Faculty of Information Technology of the University of Jyväskylä,
in the Building Villa Rana, Paulaharju Hall, on December 22, 2004 at 12 o'clock noon.

UNIVERSITY OF JYVÄSKYLÄ

JYVÄSKYLÄ 2004

Application of Mathematical Modeling for Water Environment Problems

JYVÄSKYLÄ STUDIES IN COMPUTING 47

Viatcheslav Solbakov

Application of Mathematical Modeling for Water Environment Problems

UNIVERSITY OF JYVÄSKYLÄ

JYVÄSKYLÄ 2004

Editors
Tommi Kärkkäinen
Department of Mathematical Information Technology, University of Jyväskylä
Pekka Olsbo, Marja-Leena Tynkkynen
Publishing Unit, University Library of Jyväskylä

URN:ISBN 9513920410
ISBN 951-39-2041-0 (PDF)

ISBN 951-39-2019-4 (nid.)
ISSN 1456-5390

Jyväskylä University Printing House, Jyväskylä
and ER-Paino Ky, Lievestuore 2004

ABSTRACT

Solbakov, Viatcheslav
Application of mathematical modeling for water environment problems
Jyväskylä: University of Jyväskylä, 2004, 66 p. (+included articles)
Jyväskylä Studies in Computing
ISSN 1456-5390; 47)
ISBN 951-39-2041-0
diss.

In the first part of the thesis we present a thorough analysis of pollutant dispersion in water environment and physical mechanisms of its turbulent dispersion in water. While analyzing two turbulent diffusion models we find analytically that the Richardson model with variable coefficients is substantially better in comparison with constant coefficients. Also we are interested in modeling of shot and continuous intrusion of contaminants. For the 2D transport and diffusion equation with homogeneous coefficients we manage to construct analytical solution both for shot and continuous intervention cases. The latter case is treated via a specially devised "cloud method". This method enables to account for the turbulence and "4/3" law which seems to be new for the case of continuous intervention. The method is expanded to the case of suspended solids dispersion. The case of 3D transport and diffusion equation is also considered. The solution method based on Gaussian clouds is applied to 3D transport and diffusion of sediment substances. The numerical method based on momentum approach is used for the definition of the cloud parameters. The way to introduce the "4/3" law for the 3D transport and diffusion equation in the case of substances sedimented on the bottom is also given. The approach of implementation of connection of near field and far field regions is considered. In the second part of the thesis the task of calculations of hydrodynamics parameters (sea level, current velocity and temperature distribution) is formulated for various environments based on 3D geophysical hydrodynamics equations. Special emphasis made on the circumstance that opens boundary conditions must be compatible both for the 3D and for the shallow water formulation. For a numerical solution of the three-dimensional non-stationary equations of geophysical hydrodynamics we use finite-difference equations which conserve the main variables (water and heat) and take into account the time-dependence variability of the solution area. Some illustrations and simulation results are represented for various pools and different environment conditions. The results of simulations for a short-term variability of circulation and thermal structure in Lake Jyväsjärvi are presented. Common problems arising while designing information systems are examined from the point of view of joined operation of mathematical models, data bases and Geographic information system. The problems considered here are of interest for both academic and practical applications in the field of environment modeling.

Keywords: numerical simulation, geophysical hydrodynamics, water quality, thermal structure of a Lake, finite differences, structure streamline, contamination dispersion, geographic information system

Author

Viatcheslav Solbakov
Department of Mathematical Information Technology
University of Jyväskylä
Finland

Supervisors

Professor Pekka Neittaanmäki
Department of Mathematical Information Technology
University of Jyväskylä
Finland

Dr. Boris Arkhipov
Dorodnicyn Computing Centre
of the Russian Academy of Sciences
Russia

Reviewers

Professor Anca Marinov
Bucharest University of Technology
Romania

Professor Vasiliy Dikusar
Moscow Physical Technical Institute
Russia

Opponents

Professor Jari Hämäläinen
Department of Applied Physics
University of Kuopio

Docent Joonas Hokkanen
Consulting Engineers
Paavo Ristola LTD

ACKNOWLEDGEMENTS

I wish to express my sincere gratitude to Professor Pekka Neittaanmäki and Dr. Boris Arkhipov for introducing me to the area of contemporary numerical mathematics and for their continuous attention and encouragement during the preparation of the thesis.

Several persons have made important contributions to the thesis. I am especially thankful to my colleagues Dr. Vladimir Koterov and Dr. Aleksei Marchenko for their cooperation and for their many extremely fruitful recommendations. I am also grateful to Docent Sergey Korotov for his assistance and to Dr. Kevin Rogovin and MSc. Steve Legrand for giving suggestions on how to improve the text. My thanks also to Prof. Anca Marinov and Prof. Vasiliy Dikusar for their careful review of the manuscript.

This thesis is based on the research carried out in the Department of Mathematical Information Technology of the University of Jyväskylä and previous work in the Computing Center of Russian Academy of Science. I am sincerely grateful to the staff members of these departments for providing an excellent research atmosphere and assistance at all the stages of my work. The thesis was supported by the COMAS Graduate School by Academy of Finland and by Agora Centre of the University of Jyväskylä, which support I really appriciate.

Finally, I would like to express my deepest appreciation and sincere feelings to my family for encouragement and patience.

Jyväskylä, December 13, 2004 Viatcheslav Solbakov

CONTENTS

LIST OF INCLUDED ORIGINAL PUBLICATIONS

[I] ARKHIPOV B.V., KOTEROV V.N., KOCHEROVA A.S., SOLBAKOV V.V., HUBLARIAN G.M., *Calculating sediment transport in the coastal zone of the sea,* Journal Water resources, 31, 3, 2004, pp. 27-34.

[II] TSCVETSINSKY A.S., ARKHIPOV B.V., SOLBAKOV V.V., *Tree dimensional Hydrodynamic Model of the tide and wind current in the Baidaratskaja bay of the Kara Sea,* Proceedings of the Eighth International Offshore and Polar Engineering Conference, Montreal, Canada, May 24-29, Vol.3, 1998, pp. 184-188.

[III] ARKHIPOV B.V., KOTEROV V.N., KOCHEROVA A.S., SOLBAKOV V.V., HUBLARIAN G.M., *Modeling of flow at hydraulic structures in the shelf zone of seas,* Journal Water resources, 30, 6, 2003, pp. 653-658.

[IV] TSVETSINSKY A.S., ARKHIPOV B.V., SOLBAKOV V.V., *Development of Hydrodynamic Module in the Specialized Information Analytical Systems,* The Proceedings of The Tenth International offshore and polar engineering conference, Seattle, USA, May 28- June 2, Vol. I, 2000, pp. 535-539.

[V] ARKHIPOV B.V., HUTTULA T., SOLBALKOV V.V., LINDFORS A., SEPPÄNEN J., KANGAS A., KOROTOV S., SALONEN K., *Experimental and numerical investigation of circulation and thermal structure in lake Jyväsjärvi: Short-term variability*, European Congress on Computational Methods in Applied Sciences and Engineering, ECCOMAS 2004, Finland, Jyväskylä, July 24-28, Vol. 2, 2004, pp. 1-18.

[VI] ARKHIPOV B.V., MARCHENKO A.V., SOLBAKOV V.V., *Development of the block "Ice Scouring" in Specialized Information System "Yamal"*, Proceedings of the 15th International Conference on Port and Ocean Engineering under Arctic Conditions, POAC'99, Espoo, Finland, August 23-27. Vol. 2, 1999, pp.529-536.

LIST OF SYMBOLS

ε	energy dissipation rate
ν	molecular viscosity
η	dissipative or Kolmogorov scale
e	part of energy on wave number unit
σ	variance
K_z	vertical diffusivity
K	diffusivity
u_i	velocity components
$\overline{u}_i$	average velocity components
u'	fluctuation of velocity components
$\mathbf{D}_{\vec{v}}$	a variance tensor of random current vector
C	concentration of pollutant
x_i	Cartesian coordinates
w	settlement velocity of SS
E_{ij}	unit tensor
K_{ij}	tensor of horizontal turbulent diffusion
K	horizontal diffusivity
U, V	total flux
$p(x)$	probability density function
$< x >= \int xp(x)dx$	average value
B	turbulence structure parameter
$M(z,t)$	mass density
$C_{00}, C_{10}, C_{01}, C_{11}, C_{20}, C_{02}$	moments
P	pressure
ρ	density
N_z	coefficient of vertical viscosity
τ, τ_x^0, τ_y^0	stress, and stress components

C_d	drag coefficient
ζ	free surface level
J	Jacobian
f	coriolis parameter
H, ς, h	depth
u_n, u_τ	normal and tangential component velocities
κ	Karman constant
h_w	equivalent height of a surface roughness
c	gravity waves speed
λ_i	eigenvalues
$\vec{l}$	eigenvector
l, m, n	eigenvector components
g	gravity constant
$\Phi(H,U,V)$	Riemann's invariants
x_i , y_j , z_k	grid nodes
ς^n, u^n, v^n	variables on the previous time layer
$\varsigma^{n+1}, u^{n+1}, v^{n+1}$	variables on the next time layer

LIST OF FIGURES

LIST OF TABLES

1 INTRODUCTION

1.1 Modeling for the water environment problems

One of the major goals of environmental science is to determine the spatial and temporal development of chemical constituents originating from natural or anthropogenic sources in an ecosystem. To understand and to predict the fate of such substances in seas and lakes, physical transport is one of the dominating factors. For this purpose, many numerical circulation and dispersion models have been constructed in the past. The results of the models mentioned would predict the water temperature, salinity, velocity, and density fields that are used by the plume dispersion model. The plume dispersion model simulates the passive scalars that do not influence the velocity or density fields. Further, plume models can be extended to predict water quality, ecosystem interactions, perform particle tracking, or to provide input to models that predict changes in seabed characteristics. The number of problems the researchers have to decide in environment modeling is rather enormous [14].

Near field and far field. A near-field plume model might be used to predict the near fields plume dynamics so that accurate estimates of height of rise and initial dilutions can be calculated. This would require linking the far field and near field dispersion models together (see section 2).

Boundary Conditions. The boundary conditions would include the information specified along the boundaries of the system over the complete time frame simulated. The information needed to run the model (data requirements) are expressed in terms of initial conditions, boundary conditions, and assimilated data. Both locations and types of boundary conditions are important because the information specified on the boundaries ultimately propagates through the system and must be accurate in order to model predictions to be meaningful. Boundary conditions should be set at locations where the information at the boundaries is either known (such as at shorelines), or such that the boundaries

chosen do not influence significantly the desired results in the model domain. For open boundary modeling, this can be very difficult to achieve. The types of boundary conditions that are specified can also be important. Generally, the presence of boundaries should not influence the transport of momentum, energy, or mass through them (see section 3). The modeling application to the wastewater plume that is discharged in the environment water requires the specification of an open ocean boundary condition. An open ocean boundary is the specified surrounding water boundary of the modeling domain. That is, inside the boundary, the model simulates the relevant processes to predict the hydrodynamics characteristics and the fate of the plume, and on the boundary the appropriate forcing information or boundary conditions are specified. Unfortunately, along the open lateral boundary it is not possible to specify the required information with great accuracy. Thus, the presence of an open lateral boundary condition is a real challenge for appropriate handling.

Initial Conditions and assimilated data. The initial conditions define the state of the system at the beginning of simulation. Assimilated data are those data that are continuously fed into the model as it executes, to make prognostic predictions. Such data are not needed for diagnostic simulations. Assuming the number of grid points in the dispersion model's grid is on the order of 10^4 to 10^6, then for an accurate depiction of initial conditions, data need to be available at all those locations, or a plausible interpolation of available data is needed. Of course this interpolation may not be plausible, especially the initial plume configuration. Several options are available to handle this difficulty (in addition to more intensive sampling, which is not considered here). One, the model can be run for a period long enough so that the results are independent of the initial conditions. Or two, the initial conditions are set to a plausible scenario that mimics a situation of concern in order to follow the plume's response over time to that condition.

Model Assumptions, Model Physics and Process Representations. One example of model physics (or lack of it) is described in terms of the hydrostatic assumption. In terms of process representations, the representation of turbulence is important. The assumptions made in the models need to be carefully understood to be sure that the model does not assume away an important part of the problem. For example, in some cases three-dimensional models are appropriate but in the other cases two-dimensional models, assuming an averaging over one spatial dimension, could be adequately applied. As another example, most three-dimensional models assume hydrostatic equilibrium in the vertical direction (that is, vertical accelerations are unimportant). This is typically true in the water environment, even in situations where upwelling is important. However, models with these assumptions would have difficulty in simulating the near-field around the outfall itself, since vertical accelerations are very important (outfalls are designed to produce vertical accelerations to maximize initial mixing).

The preprocessing, post processing, visualization, connection with Geographic Information System (GIS) and Database Management System (DMS). The model output can be enormously large files of model predictions. They can include time series of predictions at user-specified locations, and snapshots of the spatial distribution of scalars for different times throughout the simulation period. Such output needs to be post processed so that the results are meaningful. Ultimately, either traditional approaches can be used, or newer visualization techniques can be used to display the data three-dimensionally. The use of a state-of-the-art GIS and a connection with DMS also could be an essential part of the results obtained.

Model Grid. There are a number of models with different scales and grid resolution, which is typically simulated, and where information is generated and data is required to implement the models. The grid resolutions are specified with the intention to capture the necessary information to make the applications meaningful, but not to be so resolved that the computational time is prohibitive and the problem is never solved. This remains an issue in practically all real-world applications, despite the rapidly increasing speed of computers. One of the advantages of the finite element method that leads to its application to problems of the type examined here (where the boundaries can be quite irregular) is the ability of finite element models to accurately match those irregular boundaries [12], [13] and [24]. Finite difference techniques were viewed as inferior in terms of their ability to match these irregular boundaries. However, this has changed as finite difference techniques now employ better techniques to help match irregular boundaries [34]. In the end then, the choice of a finite element vs. finite difference model for a specific problem may not depend on how accurate the boundaries can be approximated by the different techniques (they may be equally approximated), but on how the speed of simulations compare for the same degree of accuracy.

Model Numerics and Solution Approach. Due to the computational time requirements in simulating these models, the most advanced numerical techniques with a proven record of performance are needed. Based on the experience and discussion with numerical modelers, it does not appear that all models have made the best use of numerical and programming techniques to speed the execution of those models. The execution of different models on the same problem may take on an order of magnitude range, for example. This could mean the difference between a one-day and ten-day simulation time. The solution approach is, where the numerical method may include the "discrete particle method", "cloud method", and the finite difference method, are considered among other things, for their computational efficiency.

Model Accuracy, Stability and Mass Conservation. These are concepts pertinent not only to model itself, but also to any application of that model. That is, because a model has performed well with one application, it does not mean it will automatically perform well in another application. For each model

application, the issues of accuracy and stability should be reevaluated. It is important that the dispersion model conserves mass. That is, it does not create or destroys mass artificially. An example of how mass loss could occur is by passage of the plume through the grid boundary, and return of the plume back into the domain that is simulated. The outward passage could be simulated by ignoring the turbulent flux (typically acceptable), but the inward passage would have difficulty in specifying the appropriate boundary condition. If it was specified that the incoming concentration were zero, then some mass could be lost on each cycle of any velocity reversal. To minimize this or to avoid the effect may require a grid large enough to ensure that the plume never crosses the boundaries.

Model Validation. Model validation relates to model accuracy, but is not exactly the same. Model validation refers to confirming that the code is performing exactly as intended. That is, it is bug free. Generally models are validated by comparing the numerical model against simpler analytical solutions, or even against other models that have been thoroughly evaluated (but, might be simpler, for example). Since analytical solutions are the exact solutions this may be preferred. However, since only a few analytical solutions are available to the complicated problems addressed by the numerical models, typically many validation tests that may check various components of the model are required. This work can be time consuming, and the tendency may be to minimize this effort or not to document it. In fact, this is an important step in giving the model credibility, and should not only be well documented, but should be a continuing component of model quality assurance testing as the code is updated, and other test results become available.

Model Calibration and Verification. Model calibration refers to the process of matching model results against an observed data set, and adjusting (within realistic limits) selected model coefficients until the match of observed data vs. model predictions is acceptable (typically, "acceptable" has to be defined). Then the model verification step follows, where model predictions are compared against an independent data set, where no further adjustments are made in model coefficients, and again a determination is made of whether the comparison is acceptable. There is no single set of rules on the process of calibration and verification. It is reasonable to establish the goals before the process is started, including the acceptability criterion. Modelers may disagree as to whether the calibration/verification process is application specific (validation is not), but the most conservative approach is to calibrate and verify models for each site application, and to consider this an ongoing part of modeling at a site as new data become available or modeling objectives change.

Model Maintenance and Quality Assurance/Control. It is important that models be maintained, and upgraded as the need arises. This can be costly to accomplish, and unless there is a continual source of funds available for this,

models may soon become outdated and perhaps obsolete. For example, more efficient numerics that minimize numerical dispersion and make the codes execute faster and newer types of grids are typical examples of model updates that may be needed for many models developed a decade ago. The point is that unless models are continually upgraded, they will no longer reflect the current state of the knowledge in water plume modeling.

Role of Stochastic Models in Plume Dispersion Studies. Plume dispersion modeling can either be deterministic or stochastic. Further, their equations can be solved numerically or analytically (if the equations are simplified enough). Deterministic models treat the problem in a purely deterministic sense. That is, variables are not considered as random variables, nor are the model simulations repeated multiple times within a Monte Carlo loop. Stochastic models, on the other hand, do accommodate random variables in some sense. Because of the computational expense associated with executing numerical plume dispersion models, most of the modeling that is done is deterministic. In other fields, (e.g., human health risk assessments) however, where much more simplified models can be used, Monte Carlo techniques are occasionally employed. For Monte Carlo techniques to be practical, the computational time to execute the model thousands of times (so that the solution has converged in the sense that all the information contained in the random structure of the model has been extracted) has to be manageable. For example, consider a simple plume model for a riverine discharge that takes 0.5 seconds to execute, and then is executed in a Monte Carlo loop 5000 times. This would require about 40 minutes to execute. Now, consider an ocean plume-modeling scenario that requires 2 hours to simulate. Five thousand simulations would take over a year to execute, obviously a prohibitive amount of time. Thus, Monte Carlo techniques are only practical for the simpler analytical plume dispersion models. One type of relevant model that uses the concept of randomness is a particle-tracking model. In this type of model, discrete particles are tracked, and a random dispersion component is used, so that multiple simulations of the release of the same particle (or alternatively, the release of multiple particles) result in the particles migrating to different locations. This type of modeling is sometimes used to predict whether spills will impact sensitive locations. Further these models can be run in a reverse mode in an attempt to estimate where an observed impact from the spill originated.

1.2 Outline of the thesis

In the first part we present a thorough analysis of contaminated substances (CS) dispersion in water environment and various physical mechanisms of turbulent CS dispersion in water (section 2, included Article [I]). Also, we analyze different data of CS dispersion, in particular, in offshore continental shelf region, in the internal seas, lakes and water reservoirs presented in

scientific literature. A review of modern theoretical concepts and approaches to theoretical descriptions of turbulent diffusion processes is given in section 2. We apply the well-known Richardson model of turbulent diffusion [50].

We analyze two models of CS turbulent diffusion that have respectively constant and variable diffusivities (section 2.2.8). We are primarily interested in modeling of shot and continuous intervention of contaminants respectively. Firstly we find that solutions of these two models are qualitatively different. For the case of constant coefficients we classify the solutions according to the parameters of the equation. In general the solution is a Gauss function with isolines being either circle or turned around ellipses. In particular we calculate the variation rates of the range of CS plume and substance concentrations. It turned out that the constant coefficient model predicts too fast dilution of contaminants around the source after shot intervention.

On the other hand we find analytically that the dilution rate obtained from "4/3" Richardson model with variable coefficients is substantially better. As a by product we construct the analytical solutions of transport and diffusion equation for the "4/3" Richardson model [50] in the case of shot time intrusion.

We tabulate the values of dissipation rates in different environments (sea surface with waves, deep ocean layers, bottom layers, lakes, estuaries etc.) and corresponding diffusivities (section 2.3). (It is well known that the turbulent diffusivity essentially depends on the turbulent energy dissipation rate.).

The next part (section 2.3) is devoted to the construction of the analytical solution of the 2D transport and diffusion equation with homogeneous coefficients for the suspended sedimented solids. We treat both the cases of the constant and the variable granulometric composition. We have shown that the solution of variable granulometric composition can be presented in the form of constant granulometric composition solution but with the settlement velocity depending on time.

For the 2D transport and diffusion equation with homogeneous coefficients we manage to construct analytical solution both for the shot and continuous intervention cases. The later case is treated via specially devised "cloud method". This method enables to account for the turbulence and "4/3" law which seems to be new for the case of continuous intervention.

We also analyze the case of continuous intrusion for two models of CS turbulent diffusion that have respectively constant and variable diffusivities using the "4/3" law. As previously with shot intervention we find that solutions of these two models are qualitatively different. In the variable diffusivities case the width of plume is much narrower and main the mass of the contaminant is concentrated in a narrow region. It leads to much more concentrations on the far distances from the contaminant source in comparison with the constant diffusivity case (section 2.3.2).

Additionally, the discrete particle method is also considered for the solution of transport and diffusion equation. The connection of this approach with random walking task is analyzed. The latter is the formal substantiation of the applicability of the discrete particle method for the solution of transport

diffusion equation. Some properties of the discrete particle method solutions are investigated (section 2.3.2).

The case of the 3D transport and diffusion equation is also considered. The solution method based on Gaussian clouds is applied to this task. The numerical method based on the momentum approach is used for the defining of the cloud parameters. The way to introduce the "4/3" law for the 3D transport and diffusion equation in the case of substances sedimented on the bottom is also given (section 2.3.2).

The approach of implementation of connection of near field and far field regions is considered in section 3.3.6 and 2.4.4.

The examples of calculations of plume dispersion for various practically important problems are given. They include the dredging works and discharges of contaminants from offshore objects (included Article [I]).

In the second part of the thesis the task of calculations of hydrodynamics parameters (the sea level, current velocity, and temperature distribution) is formulated for various environments. The modeling is based on application of 3D geophysical hydrodynamics equations. The connection of 3D geophysical hydrodynamics equations and equations of shallow water is demonstrated. The derivation of the latter is presented based on the transformation of Cartesian coordinates to σ coordinates system and implementation of averaging on sea depth (section 3.1).

It is shown that the coupled formulation of 3D geophysical hydrodynamics equations and equations of shallow water is an essential property of the considered task. This quality is a result of the presence in 3D formulation variables of different types that depend on independent variables in another way (section 3.1).

Based on the coupled formulation and applying of Riemann's invariants the boundary condition formulation on the open lateral boundary is given in section 3.2. It is shown that the boundary conditions should be formulated at two steps. On the first step the boundary conditions for the shallow water equations should be given in the form of Riemann's invariants. The part of them connected with characteristics incoming into solution region are given based on additional external information (the model forcing) but the other parts are calculated based on internal solution and conditions like "free issue" or :" nonreflecting conditions". At the second step the boundary conditions for the last 3D variables are formulated with special emphasis made on the moment that these conditions have to be given in accordance with formulated conditions with shallow water equations.

The description based on a finite-differences method of a numerical solution of the three-dimensional non-stationary equations of geophysical hydrodynamics is given. These finite-difference equations conserve of water mass and take into account time-dependence variability of the solution area (section 3.2.3).

Examples of calculation of a problem of circulation for different

environments of a surrounding medium are reduced. Some illustrations and simulation results are shown for various water bodies and different environment conditions (included Articles [II], [III], [V]). On the basis of the three-dimensional equations of geophysical hydrodynamics simulations of tidal circulations are performed for Baidara Bay (Kara Sea) [II]. Basic properties of tidal condition of the bay are obtained. For basic tidal waves amplitude and phase field are computed and co-tidal charts are plotted. Ellipses of tidal currents for miscellaneous parts of the Bay are calculated. The problem of flow around an artificial object in the Caspian Sea shelf is resolved on the basis of the shallow water equations [III].

Since the first famous numerical model applications by S. Uusitalo in 1960 [57], there has been significant progress in hydrodynamic modeling in Finland with numerous model applications ([55], [54], [17], [29], [52], [53], [23], [48], [58]). In most applications 2D depth integrated models have been used but the need for 3D model applications is evident for stratified lakes and the Baltic Sea [5]. The models have been used both for short-term and long-term simulation of hydrodynamic processes in lakes and the Baltic Sea together with the most important water quality variables. Calculations of thermal and hydrodynamic processes in Lake Jyväsjärvi [V] are conducted based on the oceanic circulation model of the Princeton University [35]. The process of vertical interchange in Lake Jyväsjärvi is simulated by the means of this well-known community model. At the implementation of boundary conditions the approaches given in thesis are applied.

Common problems arising while designing information systems are examined from the point of view of joined operation of mathematical models, Database Management and Geographic Information System [IV], [VI]. Considering the terminal goals of simulation in environment there is a whole set of problems needed to be solved. Environment data that are used as forcing are frequently represented in different formats. To use them in a model, it is necessary to use preset specifications. On the other hand, results of a model simulation should be presented in a user-friendly form. For the first state a database is suitable, for the second a geographic information system is useful, because frequently such data are presented as layers of the map. Interaction of parts of an information system allows using their specialized means fruitfully. The hydrodynamic model substantially described in the included Article [II] is adapted to satisfy predefined specifications to input and output data. Some results are presented in the included Article [IV]. The included Article [VI] contains comprehensive description of an interface model-database and model-GIS interaction.

1.3 Author's contribution

Author's contribution in the papers [I], [II] and [III] have been in participating of deriving of main theoretical ideas and in developing of numerical algorithms,

software, as well as in doing all practical implementation of method involved. The participation in paper [V] was expressed also in doing of computer calculations and analysis of obtained results. The results of papers [IV], [VI] have been obtained in period of working in a large project on Information System developing where author have taken a part in developing of general principles and the software modules.

2 MODELING OF TRANSPORT AND DIFFUSION OF PASSIVE CONTAMINATION IN SEA ENVIRONMENT

2.1 Introduction

The classic problem of dispersion of a passive contaminant in sea environment is interesting from different aspects. In the first place, from the theoretical view, this problem is an example of turbulence phenomena [31]. In the second place, from the practical view at last time the interest to these problems essentially increased because of realization of different projects in offshore region and implementation of environment impact assessments.

The following description is mainly concerned with dispersion of passive contaminants in seas and inshore water bodies although it also could be relevant to dispersion of contaminants in the atmosphere. On consideration of contaminant dispersion, two distinct regions, the near field and the far field could be distinguished. In the near field region the initial jet characteristics of momentum flux, buoyancy flux, and outfall geometry influence the jet trajectory and mixing. This encompasses the jet subsurface flow and any surface or bottom interaction, or in the case of a stratified ambient, terminal layer interaction. In this region, outfall design can usually affect the initial mixing characteristics through appropriate manipulation of design variables. In particular, designs with dynamic bottom attachments should be avoided.

The buoyant jet motion terminates and far-field mixing begins at the boundary interaction, at the stratified terminal layer formation with density current buoyant spreading motions, or at the moment of transition to passive diffusion due to ambient turbulence. In the far-field region, the source characteristics become less important; conditions existing in the ambient environment will control the trajectory and the dilution of the flow.

If the effluent flow contains sufficient buoyancy there will be a density current in the far field region followed by a passive diffusion region. If the effluent flow is non-buoyant or weakly buoyant there is no density current

region and only a passive diffusion region will be presented.

In this work the process of passive diffusion in the far field region which is controlled by the turbulent mixing related with ambient conditions, is analyzed. In the far field region the concentration of substances is essentially diminishing because of turbulent diffusion and settlement in case of suspended solids (SS). In the far field region the idea of superposition could be applied. It means that the contaminated plume could be considered as an ensemble of non-interacting separated "clouds" generated by a contaminant source. These clouds are moving through the water body under the influence of the currents. In moving, the dimensions of clouds grow and concentrations fall down. The concentration at an arbitrary point is the sum of the input of separate clouds.

Theoretical diffusion models describe the temporal development of the statistical properties of a concentration distribution based on the statistical properties of the velocity field that are assumed to be relevant for the mixing process. Richardson was the first to have observed the connection between the intensity of turbulent mixing and the scale of contaminated cloud. He also formulated the idea of cascade energy transferring from large eddies to smaller range. The subsequent development of these ideas can be found in the works of Kolmogorov [28] and Obuhov [39] , where the model of inertial range has been formulated. In this model the large scale where the energy is pumping into the turbulent flow is called an integral scale, designated by L, and the small scale designated by η is called the dissipative or Kolmogorov scale. From dimensional considerations it follows that $\eta \approx const\left(\nu^3/\varepsilon\right)^{1/4}$, where $\nu[cm^2/\sec]$ is the molecular viscosity and $\varepsilon[cm^2/\sec^3]$ is the energy dissipation rate.

The intermediate scale interval is called the inertial range: $\eta << \text{inertial range} << L$. In the inertial range, the power spectrum could be determined from dimensional considerations. For the energy density ($e[cm^3/\sec^2]$) per unit of the wave number ($k[1/cm]$) there is the following relation: $e = const \cdot \varepsilon^{2/3} \cdot k^{-5/3}$. An inertial range model has been used to describe the process of dispersion in turbulent flow by Batchelor [7] and to describe the diffusion experiments in the ocean by Okubo [40], Ward [59] and Ozmidov [43].

For the case of instant point source the dependence of diffusivity from cloud dimension is equivalent to the time dependence of variance. Such models have been considered in a number of a works (Ozmidov [43]). There are numerous experimental confirmations of this theory. In such models eddies larger than the cloud size are supposed to cause advection, while smaller eddies are held responsible for diffusion relative to the center of mass of the concentration distribution. If the cloud size ranges within the scales of the inertial range of the turbulence spectrum, dimensional arguments can be used to predict the cloud size to increase with time t as:

$$\sigma^2 \sim const \cdot \varepsilon \cdot t^3. \qquad (2.1.1)$$

Thus the statistical properties of the tracer distribution must be spherical symmetric; that is, the variance must have the same size in all directions.

However, vertical density stratification and the limited vertical size of a well mixed water body limit turbulence in the vertical.

For vertical diffusivity at the continental shelf the following values K_z are appropriate between 10^{-4} and 10^{-2} (Ozmidov [43]). Maximum vertical dimension of turbulent eddies is bounded by the depth of the sea, and the vertical turbulence has a forced character and in stable stratification is conditioned basically by the interaction with the water surface and bottom. Because of theoretical calculations of vertical turbulent diffusion, the spectrum of macroscopic turbulence models are applicable beginning from models of Prandl mixing length [49] and ending to multiparametric semi empirical models accounting water stratification [33], [15].

As shown by Monin and Ozmidov [36] formula (2.1.1) remains valid for two-dimensional (horizontal) isotropic turbulence if the cloud size is within the inertial range of the turbulence spectrum. Using (2.1.1) as $t = const^{-1/3}\varepsilon^{-1/3}\sigma^{2/3}$ and the relation of variance and diffusivity $\frac{d\sigma^2}{dt} = 2K$ (see below) we can obtain the horizontal diffusivity K in the form:

$$K = \frac{1}{2}\frac{d\sigma^2}{dt} = \frac{1}{2} const \cdot \varepsilon \cdot 3t^2 = const_1 \varepsilon^{1/3}\sigma^{4/3}. \quad (2.1.2)$$

The mathematical form of the inertial range model (equations (2.1.1) and (2.1.2)) suggests using a more general approach of a power law with the unknown exponent m to describe the growth of σ^2 with time:

$$\sigma^2 \sim const \cdot t^m. \quad (2.1.3)$$

In this case using $t = const^{-1/m}\sigma^{2/m}$ we see that the horizontal diffusion coefficient have the following form:

$$K = \frac{1}{2}\frac{d\sigma^2}{dt} = \frac{1}{2} const \cdot m \cdot t^{m-1} = const_1 \sigma^{2(m-1)/m}. \quad (2.1.4)$$

Note that in all these models the initial time t = 0 does not necessarily correspond to the time when a tracer was introduced to the water body as an infinitesimally small cloud ($\sigma^2 \sim 0$). If the initial tracer cloud has a finite size, t = 0 represents the hypothetical time when the tracer cloud had zero size. In fact, a more general form of (2.1.3) would be:

$$\sigma^2 \sim const \cdot (t + t_0)^m,$$

where t_0 is defined by the initial cloud size at $t = 0$: $\sigma_0^2 = const \cdot (t_0)^m$.

Okubo [40] on the basis of many different dye experiments in the surface layer of the ocean compiled the most reliable data set. He combined the results from several experiments into an ensemble of measurements and subsequently compared it to model predictions. Deviations of the data of such an ensemble from a model curve were then regarded as randomly distributed. The different environmental conditions prevailing during the different experiments were neglected. Okubo suggested that for a wide range of scales (as between 1 km and 10 km and above 10 km too) the data could be interpreted as conforming to the law $\sigma^2 \sim t^3$ and thus supporting the inertial range model. He however

stated that his interpretation based on the inertial range model is by no means decisive [40]. In some experiments the growth rate can be changed from 0.5 to 3.3 (Foxworthy et all. [18], Murthy [38] and Peeters et all. [47]). Finally, we note that the Fickian law with constant diffusivity corresponds to m = 1.

Thus, the case of instant point source has been investigated through detailed observational data and theoretical considerations. These studies lead to a power relationship of mixing rate of scale or time. Nevertheless, a priori it is not clear in what manner in the general case, continuous sources in a moving environment the effect of turbulence could be taken into account by way of appropriate definition of horizontal diffusivity of time, coordinates or other additional parameters. The present work is devoted to consideration of this question. The approach presented describes the dispersion of contaminant at a continuously effluent source. The way of accounting for turbulent diffusion intensity of scales and time is presented. The comparison of solutions in different approaches of task discretization and description of turbulent mixing is carried out.

2.2 Semi empirical turbulent diffusion equation

The velocity field of a turbulent flow can be presented as follows:

$$u_i = \overline{u}_i + u_i', \ i = 1,2,3. \tag{2.2.1}$$

Let's consider a variance tensor of a random current vector:

$$\mathbf{D}_{\vec{v}} = \begin{Bmatrix} \overline{u'^2} & \overline{u'v'} & \overline{u'w'} \\ \overline{u'v'} & \overline{v'^2} & \overline{v'w'} \\ \overline{u'w'} & \overline{v'w'} & \overline{w'^2} \end{Bmatrix}. \tag{2.2.2}$$

This tensor characterizes small scale velocity fluctuations and in general accounts for contaminant diffusion in the sea. In the two-dimensional case the tensor has the form:

$$\mathbf{D}_{\vec{v}} = \begin{Bmatrix} \overline{u'^2} & u'v' \\ \overline{u'v'} & \overline{v'^2} \end{Bmatrix}. \tag{2.2.3}$$

Owing to the symmetry of this tensor it can be reduced to a diagonal form by the rotation of the coordinate system in an angle α: $\tan 2\alpha = \dfrac{2\overline{u'v'}}{\overline{u'^2} - \overline{v'^2}}$.

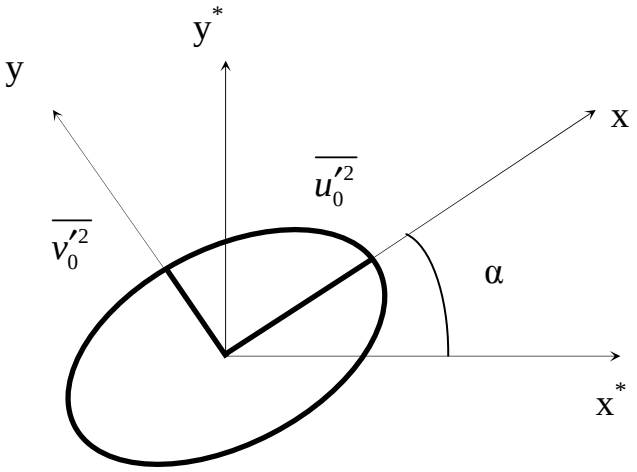

FIGURE 2.2.1: Variances of tensor of random current vector.

In simulation of transport and diffusion of passive contaminant the semi empirical equation of turbulent diffusion is widely used. This equation is obtained by the following manner. The concentration is presented by analogy with (2.2.1) as a sum of the mean value and fluctuation:

$$C = \overline{C} + C'. \tag{2.2.4}$$

The individual realizations are supposed to comply with the following conservation equation

$$\frac{\partial C}{\partial t} + \sum_1^2 \frac{\partial (u_i C)}{\partial x_i} + \frac{\partial \left((u_3 + w) \cdot C \right)}{\partial z} = 0, \tag{2.2.5}$$

where t is the time variable, x_i are the Cartesian coordinates, separated vertical coordinate $z = x_3$ measured at the gravity direction and w = const is the settlement velocity of SS (the molecular diffusivity is considered as small).

Equation (2.2.1) is averaged by an ensemble of random realizations based on Reynolds's averaging rules. The mean product of fluctuations is simulated with gradient transport hypothesis:

$$\overline{u_i' C'} = -\sum_{j=1}^{3} K_{ij} \frac{\partial \overline{C}}{\partial x_j}, \quad K_{ij} = K_{ji}. \tag{2.2.6}$$

The symmetric second rank tensor $K_{ij}, i, j = 1,2,3$, is called the tensor of turbulent diffusion. In natural conditions, it can be simplified so that the turbulent diffusion equation is read as (the lines denoting the average variable are omitted):

$$\frac{\partial C}{\partial t} + \sum_1^3 \frac{\partial (u_i C)}{\partial x_i} + w \frac{\partial C}{\partial z} = \sum_{i=1}^{2} \left[\frac{\partial}{\partial x_i} \sum_{j=1}^{2} K_{ij} \frac{\partial C}{\partial x_j} \right] + \frac{\partial}{\partial z} \left(K_z \frac{\partial C}{\partial z} \right). \tag{2.2.7}$$

The scalar value K_z is the vertical turbulent diffusivity; the values K_{ij} are the symmetric tensor of horizontal turbulent diffusion. Based on the presentation about isotropic horizontal turbulence, it is additionally supposed that

$K_{ij} = K_h E_{ij}$, where the scalar K_h is the horizontal diffusivity, but E_{ij} is the unit tensor. The last supposition is far from being always true (see below). The estimates of values K_{ij} and K_h can be implemented by the comparison of observations with solution of simplified forms of equation (2.2.7).

2.3 Depth averaged equation of transport and diffusion

2.3.1 General considerations

Let's consider the transport and diffusion of SS in a water layer of constant depth H when $u_3 = 0$, but horizontal velocity components u_1, u_2 can be dependent on only horizontal coordinates. In this case equation (2.2.7) can be read as:

$$\frac{\partial C}{\partial t} + \frac{\partial (UC)}{\partial x} + \frac{\partial (VC)}{\partial y} + \frac{w}{h} C = \frac{\partial}{\partial x} K_{xx} \frac{\partial C}{\partial x} + \frac{\partial}{\partial x} K_{xy} \frac{\partial C}{\partial y} + \frac{\partial}{\partial y} K_{xy} \frac{\partial C}{\partial x} + \frac{\partial}{\partial y} K_{yy} \frac{\partial C}{\partial y}. \tag{2.3.1}$$

In geophysical applications, the x-axis is often aligned with East and the y-axis with North.

Let's consider the problem of transport and diffusion of instant point discharge. In this case the plume is appearing. It is drifting and gradually increasing its dimension. The partial solution of initial task describing the moving of a Gaussian cloud in uniform hydrodynamic fields (all coefficients are only functions of time, but not arbitrary) has the following form (can be checked by immediate substitution):

$$G(x, y, t) = \frac{1}{2\pi S} \exp\left(-\frac{\sigma_x^2 \sigma_y^2}{S^2} \left[\frac{(x - x_0)^2}{2\sigma_x^2} + \frac{(y - y_0)^2}{2\sigma_y^2} - \frac{S_{xy} (x - x_0)(y - y_0)}{\sigma_x^2 \sigma_y^2} \right] \right), \tag{2.3.2}$$

$$\frac{dx_0}{dt} = U, \ \frac{dy_0}{dt} = V, \ \frac{d\sigma_x^2}{dt} = 2K_{xx}, \ \frac{d\sigma_y^2}{dt} = 2K_{yy}, \ \frac{dS_{xy}}{dt} = 2K_{xy}, \ S^2 = \sigma_x^2 \sigma_y^2 - S_{xy}^2. \tag{2.3.3}$$

The law of evolution of diffusivity is connected with the changing of the Gauss function and determines the evolution of contaminated substances (CS) in space and time. In general one can only say that these values are not arbitrary and should satisfy general relationships: they should not be negative, diffusion tensor should be positive definite and so on. Moreover, in practice one can consider only special cases of such a law. Below the case of constant diffusion coefficients (not changed in time and in space) and also the case of time varying

coefficients (not changed in space but with specific law of changing in time) will be considered.

Let's consider the rotation of a coordinate system on angle α determined by the following formulas:

$$\begin{aligned} &x = \cos\alpha x' - \sin\alpha y', \quad y = \sin\alpha x' + \cos\alpha y', \\ &x' = \cos\alpha x + \sin\alpha y, \quad y' = -\sin\alpha x + \cos\alpha y. \end{aligned} \tag{2.3.4}$$

With the functional connections of the initial and rotated coordinate systems we have the relationship:

$$G(x, y) = G(x(x', y'), y(x', y')) = G'(x', y'). \tag{2.3.5}$$

Owing to differentiation rules one can obtain that derivatives incoming in (2.3.1) are connected as follows:

$$\frac{\partial}{\partial x}G(x, y) = \frac{\partial G'}{\partial x'}\cos\alpha - \frac{\partial G'}{\partial y'}\sin\alpha,$$

$$\frac{\partial}{\partial y}G(x, y) = \frac{\partial G'}{\partial x'}\sin\alpha + \frac{\partial G'}{\partial y'}\cos\alpha.$$

Relations for terms containing components of tensor are:

$$K_{xx}\frac{\partial^2}{\partial x^2}G(x, y) = K_{xx}\frac{\partial^2 G'}{\partial x'^2}\cos^2\alpha - 2K_{xx}\sin\alpha\cos\alpha\frac{\partial^2 G'}{\partial x'\partial y'} + K_{xx}\frac{\partial^2 G'}{\partial y'^2}\sin^2\alpha,$$

$$2K_{xy}\frac{\partial^2}{\partial y\partial x}G(x, y)$$

$$= 2K_{xy}\sin\alpha\cos\alpha\frac{\partial^2 G'}{\partial x'^2} + 2K_{xy}\frac{\partial^2 G'}{\partial y'\partial x'}(\cos^2\alpha - \sin^2\alpha) - 2K_{xy}\sin\alpha\cos\alpha\frac{\partial^2 G''}{\partial y'^2}$$

and

$$K_{yy}\frac{\partial^2}{\partial y^2}G(x, y) = K_{yy}\sin^2\alpha\frac{\partial^2 G'}{\partial x'^2} + 2K_{yy}\sin\alpha\cos\alpha\frac{\partial^2 G'}{\partial x'\partial y'} + K_{yy}\cos^2\alpha\frac{\partial^2 G'}{\partial y'^2}.$$

Relations for transformation of velocity components and derivatives of function *G* are:

$$u' = u\sin\alpha + v\cos\alpha, \quad v' = -u\cos\alpha + v\sin\alpha,$$

$$u\frac{\partial}{\partial x}G(x, y) + v\frac{\partial}{\partial y}G(x, y) = u'\frac{\partial G'}{\partial x'} + v'\frac{\partial G'}{\partial y'}.$$

Finally, for tensor components we have the following relation:

$$K_{x'x'} = \cos^2\alpha K_{xx} + 2\sin\alpha\cos\alpha K_{xy} + \sin^2\alpha K_{yy},$$

$$K_{y'y'} = \sin^2\alpha K_{xx} - 2\sin\alpha\cos\alpha K_{xy} + \cos^2\alpha K_{yy},$$

$$K_{x'y'} = \sin\alpha\cos\alpha\left(K_{yy} - K_{xx}\right) + (\cos^2\alpha - \sin^2\alpha)K_{xy}.$$

For transformation of variances and covariance the following formulas are used:

$$\sigma_x'^2 = \cos^2\alpha\sigma_x^2 + 2\sin\alpha\cos\alpha S_{xy} + \sin^2\alpha\sigma_y^2,$$
$$\sigma_y'^2 = \sin^2\alpha\sigma_x^2 - 2\sin\alpha\cos\alpha S_{xy} + \cos^2\alpha\sigma_y^2,$$
$$S_{xy}' = \sin\alpha\cos\alpha\left(\sigma_y^2 - \sigma_x^2\right) + \left(\cos^2\alpha - \sin^2\alpha\right)S_{xy}.$$

Let's note that the parameters of a Gaussian cloud are transformed as diffusion tensor components. The following variants can be considered as the case of constant coefficients.

a) $K_{xx} = K_{yy} = K,\ K_{xy} = 0$.

In this case:
$\sigma_x^2 = \sigma^2,\ \sigma_y^2 = \sigma^2,\ S_{xy} = 0,$
$K_{x'x'} = K,\ K_{y'y'} = K,\ K_{x'y'} = 0,$
$\sigma_x'^2 = \sigma^2,\ \sigma_y'^2 = \sigma^2,\ S_{xy}' = 0.$

The solution is a rotation symmetric Gauss function. The isolines of it are circles.
b) $K_{xx} \neq K_{yy}$; (for distinctness $K_{xx} > K_{yy}$), $K_{xy} = 0$.

In this case:
$\sigma_x^2 = 2K_{xx}(t - t_0),\ \sigma_y^2 = 2K_{yy}(t - t_0),\ S_{xy} = 0.$
The solution doesn't have rotation symmetry. The isolines are ellipses. For tensor components we have the following relation:
$K_{x'x'} = \cos^2\alpha K_{xx} + \sin^2\alpha K_{yy},$
$K_{y'y'} = \sin^2\alpha K_{xx} + \cos^2\alpha K_{yy},$
$K_{x'y'} = \sin\alpha\cos\alpha\left(K_{yy} - K_{xx}\right).$
Variances and covariance in this case are:
$\sigma_x'^2 = \cos^2\alpha\sigma_x^2 + \sin^2\alpha\sigma_y^2,$
$\sigma_y'^2 = \sin^2\alpha\sigma_x^2 + \cos^2\alpha\sigma_y^2,$
$\sigma_y'^2 = \sin^2\alpha\sigma_x^2 + \cos^2\alpha\sigma_y^2.$
The axes of the initial coordinate system are oriented along the axes of an ellipse. It means that the rotation transforms the diffusion tensor and quadratic matrix to nondiagonal form.
c) $K_{xx} = K_{yy} = K,\ K_{xy} \neq 0.$
In this case:
$K_{x'x'} = K + 2\sin\alpha\cos\alpha K_{xy},$
$K_{y'y'} = K - 2\sin\alpha\cos\alpha K_{xy},$
$K_{x'y'} = (\cos^2\alpha - \sin^2\alpha)K_{xy}.$
Variances and covariance in this case are:

$\sigma_x'^2 = \sigma^2 + 2\sin\alpha\cos\alpha S_{xy}$,

$\sigma_y'^2 = \sigma^2 - 2\sin\alpha\cos\alpha S_{xy}$,

$S_{xy}' = \left(\cos^2\alpha - \sin^2\alpha\right) S_{xy}$.

The rotation by the angle α ($\cos 2\alpha = 0, \alpha = 45^\circ$) leads the diffusion tensor and matrix to a diagonal form. The Gauss function will have the form rotated at $\alpha = 45^\circ$ relatively initial coordinate system.

d) $K_{xx} \neq K_{yy}$ (for distinctness $K_{xx} > K_{yy}$), $K_{xy} \neq 0$.

It is the general case. Owing to previous considerations the angle α exists and is determined by the following ratio:

$$\tan 2\alpha = \frac{2S_{xy}}{\sigma_x^2 - \sigma_y^2} = \frac{2K_{xy}}{K_{xx} - K_{yy}}.$$

The rotation on the angle α leads the diffusion tensor and matrix to a diagonal form. The Gauss function will have the isolines as ellipses rotated on α relative to the initial coordinate system.

2.3.2 Discrete particles method

2.3.2.1 The formulation of method

The discrete particle method of calculation of CS dispersion in the sea is based on theoretical considerations of the random walking method analyzed by Karl Pearson (Pearson, 1905, [45]). A walker makes steps of a fixed length α and at a random angle θ (in 2-D polar coordinates) after each time interval Δt. Where is the walker after N steps? The probability density function (PDF) in the limit $N \to \infty$ has the asymptotic form,

$$p(r, N) \sim \frac{1}{N}\exp\left(\frac{-r^2}{2N}\right).$$

The scaling $\langle r \rangle \sim \sqrt{N}$ is very common for random walks. If the position is simply the sum of a large number of independent random displacements, this scaling and the shape of the distribution come naturally out of the Central Limit Theorem (CLT).

It turns out that diffusion problems are closely related to the random walk discussed above. The connection is not incidental. In fact it is possible to show that the concentration of simple random walkers approximately obeys the diffusion equation as their number becomes large, at time scales and length scales greatly exceeding those of a single step. Because the walkers are independent, this is equivalent to the limit of $p(X_N)$ as $N \to \infty$. As a tentative justification for this equivalence, consider a large number M of independent random walkers starting at x = 0 (i.e. $x(t=0) = \delta(0)$. After each is allowed to take a sufficiently large number of steps $N=t/\Delta t$ on average we will find $p(X_N)M$ walkers in $(x, x+\Delta x)$. We have already found that $p(X_N)$ is a Gaussian. A more

formal derivation is outlined below. Let $p(\Delta x) = PDF$ (probability density function) for each step Δx. $P_N(x) = PDF\ for\ X_N$. The independence of the steps can be expressed as

$$P_{N+1}(x) = \int_{-\infty}^{+\infty} p(\Delta x) P_N(x - \Delta x) d\Delta x .$$

This equation states the independence of *N*-th step from the previous history of the walk. Since Δx is assumed to have a finite variance σ^2, and X_N will have a variance that scales with *N*, we expect that $\Delta x \ll x$ as $N \to \infty$. Thus, Taylor-expanding P_N can be applied:

$$P_{N+1}(x) \approx \int_{-\infty}^{+\infty} p(\Delta x) \left[P_N(x) - \Delta x P_N'(x) + \frac{1}{2} \Delta x^2 P_N''(x) + ... \right] d\Delta x .$$

Taking the derivatives of $P_N(x)$ outside the integral we obtain:

$$P_{N+1}(x) \approx P_N(x) \int p(\Delta x) d\Delta x - P_N'(x) \int \Delta x p(\Delta x) d\Delta x + \frac{1}{2} P_N''(x) \int \Delta x^2 p(\Delta x) d\Delta x + ...$$

Hence:

$$P_{N+1}(x) \approx P_N(x) - P_N'(x) \langle \Delta x \rangle + \frac{1}{2} P_N''(x) \langle (\Delta x)^2 \rangle + ...$$

We now introduce time as a variable by stating that the steps are taken after each time interval. Thus, from the above equation we obtain:

$$\frac{P_{N+1}(x) - P_N(x)}{\Delta t} + \frac{\langle \Delta x \rangle}{\Delta t} P_N'(x) = \frac{1}{2} P_N''(x) \frac{\langle (\Delta x)^2 \rangle}{\Delta t} .$$

For small Δt we obtain approximately:

$$\frac{\partial P_N(x,t)}{\partial t} + U \frac{\partial P_N(x,t)}{\partial x} = D \frac{\partial^2 P_N(x,t)}{\partial x^2},$$

where $U = \frac{\langle \Delta x \rangle}{\Delta t}$, $D = \frac{1}{2} \frac{\langle (\Delta x)^2 \rangle}{\Delta t}$ and $t = N \Delta t$.

Note, than when $\langle \Delta x \rangle = 0$ we recover the diffusion equation, otherwise the equation describes diffusion in a medium flowing with a drift velocity. This is called an *advection-diffusion* problem, advection referring to the flow term. Thus, we see a clear relation between the macroscopic phenomenon of diffusion and the underlying microscopic phenomenon of the random walk a similar approach in two-dimensional case leads to the following equation:

$$\frac{P_{N+1}(x,y,t) - P_N(x,y,t)}{\Delta t} + \frac{\langle \overrightarrow{\Delta r} \rangle}{\Delta t} \nabla P_N(x,y,t)$$

$$= \frac{1}{2} \left(\frac{\partial^2 P_N(x,y,t)}{\partial x^2} \frac{\langle (\Delta x)^2 \rangle}{\Delta t} + 2 \frac{\partial^2 P_N(x,y,t)}{\partial x \partial y} \frac{\langle (\Delta x \Delta y) \rangle}{\Delta t} + \frac{\partial^2 P_N(x,y,t)}{\partial y^2} \frac{\langle (\Delta y)^2 \rangle}{\Delta t} \right),$$

$$\frac{\partial P_N(x,y,t)}{\partial t} + \vec{U}\frac{\partial P_N(x,y,t)}{\partial \vec{r}} = K_{xx}\frac{\partial^2 P_N(x,y,t)}{\partial x^2} + 2K_{xy}\frac{\partial^2 P_N(x,y,t)}{\partial x \partial y} + K_{yy}\frac{\partial^2 P_N(x,y,t)}{\partial y^2}, \quad (2.3.6)$$

where $\vec{U} = \frac{\langle \overrightarrow{\Delta r} \rangle}{\Delta t}$, $K_{xx} = \frac{1}{2}\frac{\langle (\Delta x)^2 \rangle}{\Delta t}$, $K_{yy} = \frac{1}{2}\frac{\langle (\Delta y)^2 \rangle}{\Delta t}$, $K_{xy} = \frac{1}{2}\frac{\langle \Delta x \Delta y \rangle}{\Delta t}$ and $t = N\Delta t$.

The given considerations are the formal rationalization of the possibility of using a discrete particle method for the calculation of CS dispersion. Many variations on the random walk problem can be considered in the class, each of which can invalidate the CLT and produce 'anomalous diffusion' with different scaling behavior, not described by the simple diffusion equation in the continuum limit.

2.3.2.2 The example of calculation by discrete particles method

It is evident that the discrete particle method in the form of (2.3.6) can be used only for the transport diffusion equation with constant coefficients. Some results of calculations of SS dispersion by discrete particle method are given in Figure 2.3.1. In simulations the following parameters were used: water depth 10m, current velocity 0.1 m/sec from west to east, diffusivity equal to 2.5 m^2/sec, the source intensity 1 Kg/sec, the mass of particles 0.02 Kg that corresponds 50 particles/s., the duration of calculations 5000 s.

The calculation results show that the plume is oviform rather than with wide cross section. It is clear that this result is consistent with the constant diffusion calculations (see below, Figure 2.3.4.a).

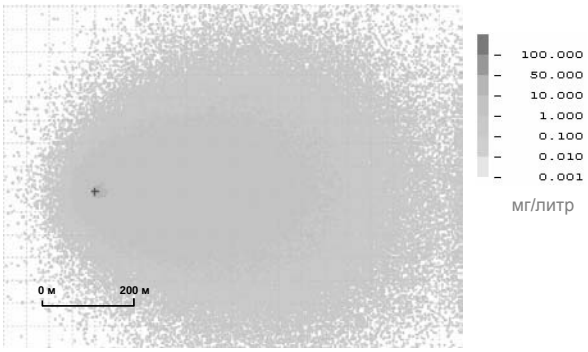

FIGURE 2.3.1: Concentration field of SS calculated by discrete particles method.

2.3.3 Method of clouds

In this section we consider the dispersion of SS in the far field zone based on the cloud method. In the case where dimension of contaminant plume is much more than the depth of water the two-dimensional depth averaged model can be used. The supposition can be made that after the near field region, the plume

acquires the form of an ellipse and the initial concentration field has a Gauss function form, which can be written in coordinate system the *x-y* rotated at angle α relative to the initial coordinate system x^*, y^* (Figure 2.3.2.) as

$$C_0(x,y) = \frac{M_i}{h} \cdot \frac{1}{2\pi\ \sigma_{0x}\sigma_{0y}}\ \exp\left(-\left(x^2 \Big/ 2\sigma_{0x}^2 + y^2 \Big/ 2\sigma_{0y}^2\right)\right)\ . \tag{2.3.7}$$

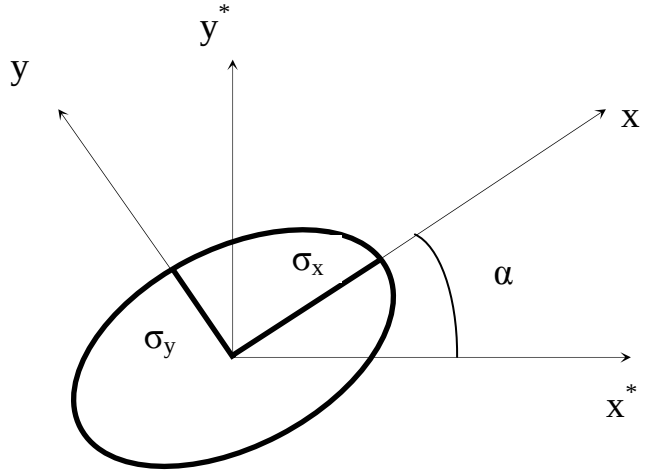

FIGURE 2.3.2: Coordinate system connected with axes of the initial ellipse.

The expression for solution can be obtained by reverse transformation on α:

$$x^* = \cos\alpha x - \sin\alpha y,\ \ y^* = \sin\alpha x + \cos\alpha y\ , \tag{2.3.8}$$

then the form of (2.3.7) will be

$$C_0(x^*,y^*) = \frac{M_i/h}{2\pi S_0}\ \exp\left(-\frac{\sigma_{0x^*}^2\sigma_{0y^*}^2}{S_0^2}\left[\frac{x^{*2}}{2\sigma_{0x^*}^2} + \frac{y^{*2}}{2\sigma_{0y}^2} - \frac{S_{0x^*y^*}x^*\cdot y^*}{\sigma_{0x^*}^2\sigma_{0y^*}^2}\right]\right)\ , \tag{2.3.9}$$

$$\begin{aligned} &S_0^2 = \sigma_{0x^*}^2\sigma_{0y^*}^2 - S_{0x^*y^*}^2\ , \\ &\sigma_{0x}^{*2} = \cos^2\alpha\ \sigma_{0x}^2 + \sin^2\alpha\ \sigma_{0y}^2,\ \ \sigma_{0y}^{*2} = \sin^2\alpha\ \sigma_{0x}^2 + \cos^2\alpha\ \sigma_{0y}^2, \\ &S_{0xy}^* = \sin\alpha\cos\alpha(\sigma_{0x}^2 - \sigma_{0y}^2). \end{aligned} \tag{2.3.10}$$

The evolution of the separate fraction *i* of the cloud SS in a coordinate system rotated parallel to the initial orientation of the cloud is described by the following equations:

$$\begin{aligned} &\frac{\partial C_i}{\partial t} + \frac{\partial(u_x C_i)}{\partial x} + \frac{\partial(u_y C_i)}{\partial y} + \frac{W_i}{h}C_i = \frac{\partial}{\partial x}K_{xx}\frac{\partial C_i}{\partial x} + \frac{\partial}{\partial y}K_{yy}\frac{\partial C_i}{\partial y}, \\ &\frac{\partial m_i}{\partial t} = W_i C_i. \end{aligned} \tag{2.3.11}$$

At small concentrations the dispersion of SS can be presented as an ensemble of non-interacting clouds, born by instant sources of mass. Based on these clouds the coming in of substances from the near field region to the far field region is simulated. These clouds are moving through the water body under the impact of currents and settle on the bottom. In moving, the cloud dimension is increased and their concentration is falling down. The concentration at an

arbitrary point of the water area is the sum of the inputs of separate clouds concentrations including the point considered at the current time moment.

The solution of (2.3.11) for a separate cloud (i – sediment fraction) can be presented as:

$$C_i = \frac{M_i}{h} G(x, y, t) \exp\left(-\frac{W_i}{h} t \right). \tag{2.3.12}$$

Here M_i is the initial mass of the i'th fraction in the cloud and the function G is similar for all the fractions describing the conservative dispersion of unit mass cloud and satisfing the following condition:

$$\frac{\partial G}{\partial t} + \frac{\partial (uG)}{\partial x} + \frac{\partial (vG)}{\partial y} = \frac{\partial}{\partial x} K_{xx} \frac{\partial G}{\partial x} + \frac{\partial}{\partial y} K_{yy} \frac{\partial G}{\partial y},$$
$$\int_{-\infty}^{\infty} \int_{-\infty}^{\infty} G(x, y, t)\, dxdy = 1 \quad . \tag{2.3.13}$$

If u, v, K_{xx}, K_{yy} don't depend on the coordinates x, y and only change with time, then the solution of equation (2.3.13) has the Gauss form

$$G(x, y) = \frac{1}{2\pi\ \sigma_x \sigma_y}\ \exp\left(-\frac{\left(x - x_u\right)^2}{2\sigma_x^2} + \frac{\left(y - y_v\right)^2}{2\sigma_y^2} \right), \tag{2.3.14}$$

where x_u, y_v (cloud center coordinates) and variances σ_x, σ_y satisfy the equations

$$\frac{dx_u}{dt} = u_x, \ \frac{dy_v}{dt} = u_y, \ \frac{d\sigma_x^2}{dt} = 2K_{xx}, \ \frac{d\sigma_y^2}{dt} = 2K_{yy}. \tag{2.3.15}$$

According to the law of "4/3", the turbulent diffusion tensor components depend on the linear dimensions $2\sigma_x$ and $2\sigma_y$ of the cloud and can be written in the following form [37], [43]

$$K_{xx} = B\left(2\sigma_x\right)^{4/3}, \ K_{yy} = B\left(2\sigma_y\right)^{4/3}, \ B = b\varepsilon^{1/3}, \tag{2.3.16}$$

where $\varepsilon[cм^2/c^3]$ is the energy dissipation rate, B is the turbulence structure parameter and $b \in [0.1, 0.2]$ ([37], p. 501). In some cases, the value of B is $4.5 \cdot 10^{-4}$ $m^{2/3}$/sec (see *Bao-Shi-Shiau at al.* [6], Ozmidov, [43]). Typical values of ε and B for various environment conditions and different lake regions are presented in Table 2.3.1. and in Figure 2.3.3.

TABLE 2.3.1: Typical values of turbulent energy dissipation rate in different conditions of sea environment.

Conditions of sea environment	Range of energy dissipation rate, ε [m^2/sec^3]	Typical value of energy dissipation rate, ε [m^2/sec^3]	Turbulence structure parameter, B, [$m^{2/3}$ / sec]
Deep sea	[10^{-7}, 10^{-5}]	10^{-7}	$4.64 \cdot 10^{-4}$
Estuary	[10^{-4}, 10^{-3}]	10^{-4}	$7.94 \cdot 10^{-3}$
Surface layer	[10^{-3}, 10^{-2}]	$5 \cdot 10^{-3}$	$1.71 \cdot 10^{-2}$
Breaking wave	[1, 10]	5	$1.71 \cdot 10^{-1}$

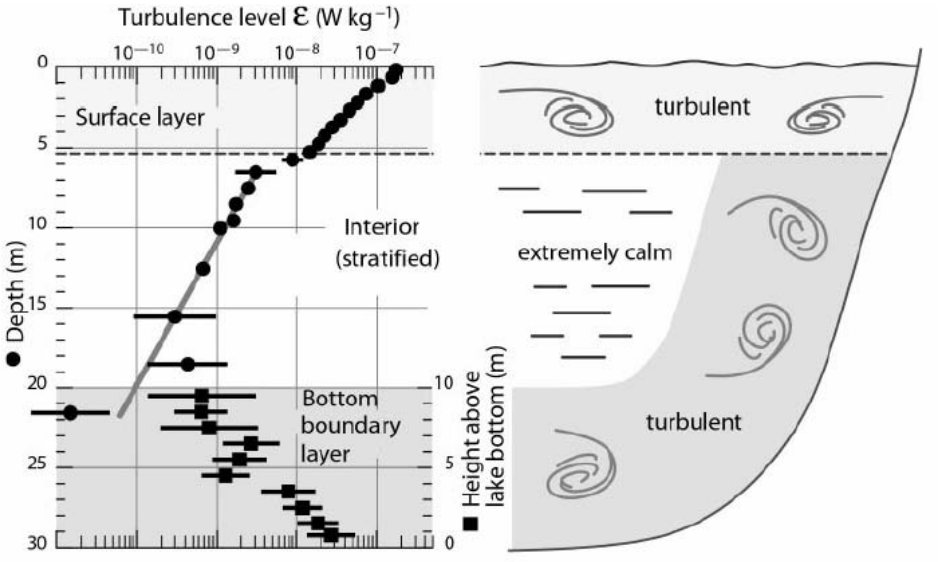

FIGURE 2.3.3: Level of turbulence in a medium-sized lake, expressed by dissipation of turbulent kinetic energy, as a function of depth (circles) and as a function of height above bottom (squares). The plot characterizes the three distinctly different water bodies separately: the energetic surface boundary layer, the slightly less turbulent bottom boundary, and the strongly stratified and almost laminar interior. Adapted from Wuest et al. [60].

For defining the variances and center mass coordinates the following initial values can be formulated:

$$\begin{aligned} &\frac{d\sigma_x^2}{dt} = 2B\left(2\sigma_x\right)^{4/3},\ \sigma_x(t=0) = \sigma_{0x}, \\ &\frac{d\sigma_y^2}{dt} = 2B\left(2\sigma_y\right)^{4/3},\ \sigma_y(t=0) = \sigma_{0y}, \\ &\frac{dx_u}{dt} = u,\ \frac{dy_v}{dt} = v,\ x_u(t=0) = 0,\ y_v(t=0) = 0. \end{aligned} \tag{2.3.17}$$

The solution of these equations has the form:

$$\sigma_x^2 = \left[\frac{2^{7/3}}{3} B\cdot\left(t-t_0\right)+\sigma_{x0}^{2/3}\right]^3,\ \sigma_y^2 = \left[\frac{2^{7/3}}{3} B\cdot\left(t-t_0\right)+\sigma_{y0}^{2/3}\right]^3,$$
$$x_u = \int_0^t u dt',\quad y_v = \int_0^t v dt'. \tag{2.3.18}$$

For the constant coefficients we have:

$$\sigma_x^2 = 2K_{x0}t+\sigma_{x0}^2,\ \ \sigma_y^2 = 2K_{y0}t+\sigma_{y0}^2.$$

The values of the horizontal diffusivities the in shelf region according to measurements are in the range $5\cdot10^{-2}$ to $4\cdot10^{4}$ $м^2/с$ (*Koh at al.* [26]). Note that the value of the vertical diffusivity coefficient K_z is from 10^{-6} to $3\cdot10^{-2}$ $м^2/с$ (*Koh at al.* [27]). In Table 2.3.2 the values of horizontal diffusivities are given for different conditions of environment and typical scales of contaminated plume, calculated by relations (2.3.16).

TABLE 2.3.2: Comparison of diffusivities for different environment conditions.

Conditions of sea environment	Typical value of energy dissipation rate, ε [m^2/sec^3]	Turbulence structure parameter, B, [$m^{2/3}/sec$]	σ_x [m]	σ_y [m]	K_x [m^2/sec]	K_y [m^2/sec]
Deep sea	10^{-6}	$1.5\cdot10^{-3}$	6	3	$4.12\cdot10^{-2}$	$1.64\cdot10^{-2}$
Estuary	$5\cdot10^{-4}$	$1.2\cdot10^{-2}$	6	3	$3.3\cdot10^{-1}$	$1.31\cdot10^{-1}$
Surface layer	$5\cdot10^{-3}$	$2.6\cdot10^{-2}$	6	3	$7.14\cdot10^{-1}$	$2.83\cdot10^{-1}$
Breaking wave	5	$2.6\cdot10^{-1}$	6	3	7.14	2.83

After the determination of the function G in a coordinate system connected with the initial orientation of the ellipse it can be expressed in starting system by the means of equations (2.3.9)-(2.3.10). Let's note that application of (2.3.16) for deducing of diffusivities the nonlinearity of problem was introduced. It should be mentioned that while using the "4/3" model we can obtain two solution types. As it follows from (2.3.18) in the first case, starting from a singular state or zero diffusivity values and Gauss function parameters the solution is symmetrical relative to rotations and the isolines have a circle form at all time. In this case it is not necessary to use a rotated coordinate system. In the second case, when the start is implemented from an initial Gauss function rotated on angle α the chosen coordinate system is introduced, so the isolines have the main axes along the coordinate axes.

2.3.4 Accounting of multi component composition of suspended solids

The fractional composition of SS becomes apparent in the differential manner of settlement of various fractions. The sum concentration evidently is equal to

$C = \sum_i C_i$, where C_i satisfies (2.3.11).

Summing (2.3.11) on all sediment fractions one can find that C will also satisfy (2.3.11) if effective hydraulic coarseness (hydraulic coarseness characterizes the size of particles and is determined by settlement velocity) W is taken in the following manner:

$$W = \sum_i (W_i C_i) \Big/ \sum_i C_i \ .$$

Here C_i of each component satisfies ratio (2.3.12), and:

$$W = W(t) = \sum_i \frac{M_i}{M} W_i \exp\left(-\frac{W_i}{h} t\right) \Big/ \sum_i \frac{M_i}{M} \exp\left(-\frac{W_i}{h} t\right), \quad M = \sum_i M_i \ , \tag{2.3.19}$$

here M is the initial mass of the cloud.

Thus the problem of simulation a of multi component cloud moving in the two dimensional case, is reduced to the calculation of dispersion of SS with mono fraction composition, but with the settlement velocity dependent on time (2.3.19). The space–time evolution of concentration in the initial orientation coordinate system will be described by the following equation similar to (2.3.11).

$$\frac{\partial C}{\partial t} + \frac{\partial (u_x C)}{\partial x} + \frac{\partial (u_y C)}{\partial y} + \frac{W}{h} C = \frac{\partial}{\partial x} K_{xx} \frac{\partial C}{\partial x} + \frac{\partial}{\partial y} K_{yy} \frac{\partial C}{\partial y} \ . \tag{2.3.20}$$

The SS concentration, the mass of laid-down SS and the thickness of sediments, evidently can be described in the following manner:

$$C = \frac{M}{h} G(x, y, t) \exp\left(- \int_{t_0}^{t} \frac{W(t' - t_0)}{h} dt' \right), \quad \frac{\partial m}{\partial t} = WC, \quad h_S = \frac{m}{(1-\delta)\rho}, \tag{2.3.21}$$

here t_0 is the time moment of the cloud birth, δ is the bottom sediment porosity, ρ is the mineral density, and G satisfies equation (2.3.13).

2.3.5 Continuity source

We now consider the continuity source of intensity $\dot{M}$ and present its operation as aggregates of point discharges functioning from 0 to t. Concentration distribution in space and time is expressed by the formula:

$$C(x, y, t) = \int_0^t \left(\frac{\dot{M}}{h} G(x, y, t - t_0) \exp\left(- \int_{t_0}^{t} \frac{W(t' - t_0)}{h} dt' \right) \right) dt_0 \ . \tag{2.3.22}$$

In such a presentation, the idea is expressed that dispersion of CS occurs

as an ensemble of Gaussian clouds and the concentration is presented as a sum of separate cloud inputs. Actually, such an expression is acceptable in suggestion of task linearity and as a consequence of the solution additivity.

The next step is the expansion (2.3.22) to take into account the "4/3" model for turbulent diffusivity. It should be noted, that the solution in the form (2.3.22) is not a solution for transport – diffusion equation in the form (2.3.20) – and it is a separate, more complex model of CS dispersion.

Two variants could be here similar to the instant point discharge. In the first case the cloud born in each time moment has infinitesimal dimensions. In this case the evolution is implemented from a symmetrical Gauss function. In the second case the time axis is divided into a number of intervals and so the cloud mass and initial dimensions are defined.

Let's consider the dispersion of SS from an isotropic point source in a constant flow velocity $u_x=U=const$, $u_y=0$. The fundamental solution of the equation (2.3.20) for a motionless medium ($U=0$) has the form:

$$G_0(x,y,t)=\frac{1}{2\pi h\sigma^2(t)}\exp\left(-\frac{x^2+y^2}{2\sigma^2(t)}-\frac{W}{h}t\right),\ \frac{d\sigma^2(t)}{dt}=2K,\ t>0. \tag{2.3.23}$$

This formula describes the dispersion of SS from the instant isotropic point source of a unit mass placed in the point of origin $x=0$, $y=0$ (W – settlement velocity, h – water depth). It should be noted that the diffusion is isotropic in the case $K_{xx}=K_{yy}=K$, $K_{xy}=K_{yx}=0$ and σ^2 is the square of a typical cloud radius. The distribution of SS from continuous point source activated at the moment $t=0$ in moving flow can be presented as a superposition of instant point sources:

$$C(x,y,t)=\int_0^t\frac{\dot{M}}{h}G_0(x-x_0,y,t-t_0)\,dt_0,\quad x_0=U\,t_0. \tag{2.3.24}$$

Here $\dot{M}$ is the source intensity (kg/sec) and G_0 is determined by the formula (2.3.23). Passing to the variable $t_1=t-t_0$ we shall obtain the expression for the concentration distribution from a motionless point source of constant intensity.

$$C=\frac{\dot{M}}{2\pi h}\int_0^t\exp\left(-\frac{(x-U\,t_1)^2+y^2}{2\sigma^2(t_1)}-\frac{W}{h}t_1\right)\frac{dt_1}{\sigma^2(t_1)},\quad t_1=t-t_0. \tag{2.3.25}$$

As it already have been noted in the case of turbulent diffusion the diffusivity consistent with of the "4/3" law has the form $K=B(2\sigma)^{4/3}$. Then from (2.3.18) we obtain:

$$\sigma^2(t_1)=(128/27)(Bt_1)^3. \tag{2.3.26}$$

Let's also consider the case of usual diffusion when K=const. In this case

$$\sigma^2(t_1) = 2K\,t_1 . \qquad (2.3.27)$$

Below we shall estimate the scales of values and compare two cases with a constant diffusivity K≈2,5 m²/sec and a turbulent diffusivity with B≈0.5·10^{-3} m$^{2/3}$/sec. The source intensity will have $\dot{M}$ =1 kg/sec, depth h=10 m and U=0.1 m/sec. For comparison purposes the settlement velocity will be taken as zero. For small fractions with the character particle diameter equal to 1 micron the settling velocity is equal to 10^{-6} m/sec, for mean fraction with character particle diameter equal to 50 micron the settling velocity is in the order of 10^{-3} m/sec. In Table 2.3.3. calculated variants are listed.

TABLE 2.3.3: The calculated variants for continuous source.

Variant	K_x, m²/sec	K_y, m²/sec	σ_{0x}, m	σ_{0y}, m	$\dot{M}$, kg/sec	T, sec	U, m/sec	W, m/sec
I	2,5	2,5	6	3	1	20 000	0,1	0
II	$B(2\sigma_x)^{4/3}$	$B(2\sigma_y)^{4/3}$	6	3	1	20 000	0,1	0
III	2,5	2,5	4	2	1	20 000	0,1	0
IV	$B(2\sigma_x)^{4/3}$	$B(2\sigma_y)^{4/3}$	4	2	1	20 000	0,1	0
V	2,5	2,5	4	2	1	5 000	0,1	0
VI	$B(2\sigma_x)^{4/3}$	$B(2\sigma_y)^{4/3}$	4	2	1	5 000	0,1	0

The variants are differed by the initial spot dimensions and also by the dependence type of diffusivity of time. For all variants the environment conditions were similar (h=10 m, U= 0,1 m, $B = 0.5\cdot10^{-3}$ m$^{2/3}$/sec. Dependencies of concentration on the x-coordinate for the two constant values of coordinate y (y=0 and y=10 m) at the time moment 20000 s. (from the activation of source) are presented in Figure 2.3.4. From the comparison it can be seen that the dilution of contaminant is much faster in the case of constant diffusivity (red curves) than in the case of "turbulent" diffusivity (black curves). The "concentration jet" in the case of turbulent diffusivity is much narrower than in the case of constant diffusivity. A similar conclusion can be made from the field pictures shown in Figure 2.3.5. for the time 5000 sec. Based on the calculations the conclusion can be made that in the case of the two models of turbulent mixing (constant diffusivity and turbulent diffusivity) the obtained results are qualitatively distinctive.

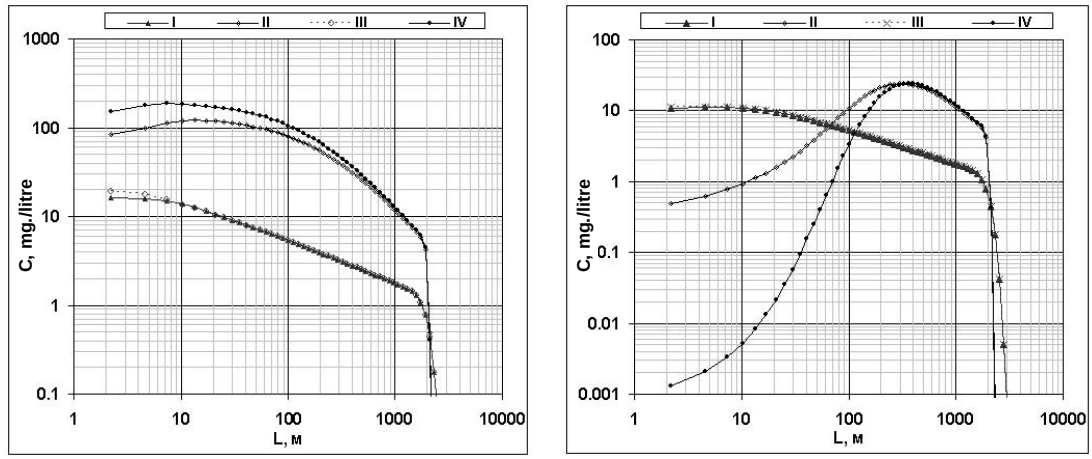

FIGURE 2.3.4: Concentration dependence on coordinate x for continuous source at y=0 m (a) and y=10 m (b).

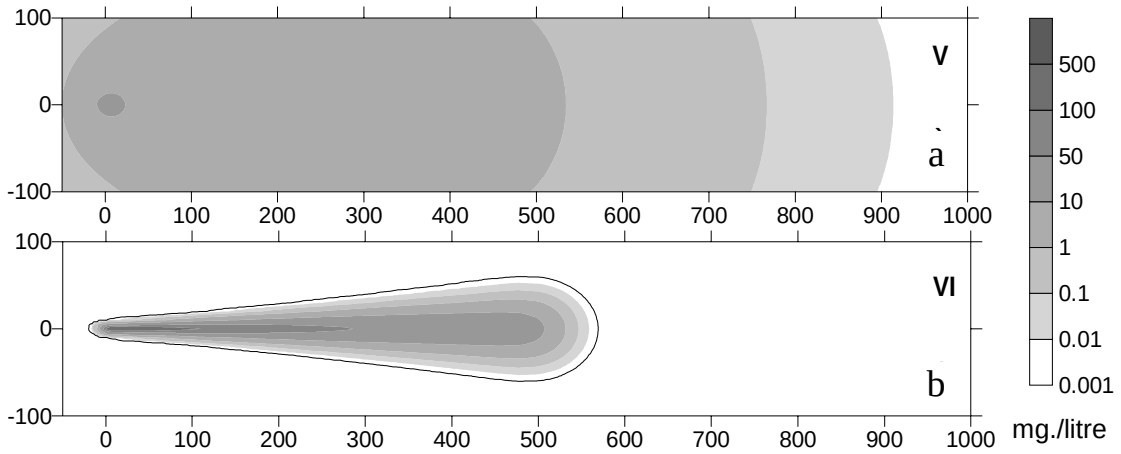

FIGURE 2.3.5: Concentration fields at constant diffusivity (a) and turbulent diffusivity (b).

2.3.6 Formation of SS clouds in the near field region

The time-space evolution of SS concentration in a far field region should not depend essentially on the concrete details, typical for the phenomenon in a near field region. It can be described only by its integrated characteristics, such as the total mass of SS and mass flow rate into seawater. In this section, the algorithm of forming separate SS clouds is presented. It can be used for the simulation of spreading production discharges, to calculate the pollution during dredging (Figure 2.3.6).

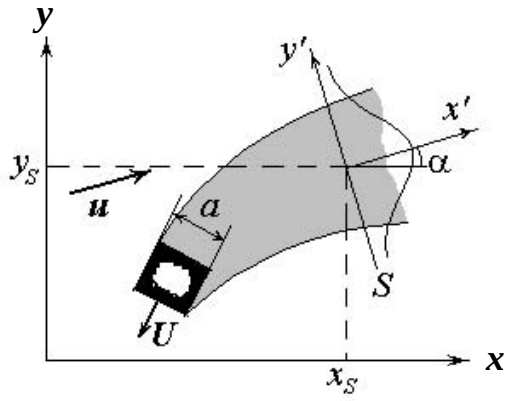

FIGURE 2.3.6: Scheme of initial clouds forming.

The plume of suspended matter within some distance from the source (in section *S* with center in coordinates x_S, y_S, see Figure 2.3.5.) is turned towards the current direction. As the velocity in the contaminated area (in the cloud interior) comes nearer to the ambient current speed *u*, the concentration C_0 on the axis of the plume falls. Furthermore the transversal distribution of the concentration *C* of SS in the plume as a result of turbulent intermixing becomes close to a Gaussian distribution with semi-axis of $\sigma_{y'}$.

Let *Q* denote the mass flowrate of the SS incoming into seawater as a result of some operation and ξ_Q the mass fraction of particles of the dredge cloud escaping the plume at the expense of sedimentation processes. Then by virtue of the mass conservation law we obtain:

$$uh\int_{-\infty}^{\infty} C dy' = (1-\xi_Q)Q,$$

therefore: $C_0 = \left(1-\xi_Q\right) \; Q \Big/ \left(\sqrt{\pi} uh\sigma_{y'}\right)$.

Let us consider a rather small time period τ_c. We assume that SS clouds will be formed in a certain point (x_S, y_S) sequentially every τ_c period. Then the sediment mass, which is to be assigned to a separate cloud, is defined by the formula: $M = (1-\xi_Q)\cdot Q\tau_c$. The reference size of this cloud in the y'-direction is to be equal to the semi-axis of the plume $\sigma_{y'}$ and the reference size of the cloud $\sigma_{x'}$ in x' direction is selected so that the concentration in the cloud center is equal to C_0. As a result we receive:

$$\sigma_{x'} = \frac{1}{\sqrt{\pi}} u \quad \tau_c .$$

Thus, according to the described algorithm, the initial characteristics of a suspended matter cloud at the given interval τ_c depend on the following parameters: the cloud center coordinates x_S, y_S, its semi-axis $\sigma_{y'}$ and the mass fraction ξ_Q of the dredge which are settled throughout the lateral area of a plume.

Special models of the jet flow can be applied for the estimation of these parameters for the practical simulation of SS discharges (Brandsma M.G. et all [9], 1992; Arkhipov B.V., Koterov V.N., Solbakov V.V., 2000 [4]). It should be noted, that the similar flow substantially depends on the magnitude and mutual orientation of the current velocity vector $\boldsymbol{u}$ and velocity $\boldsymbol{U}$ in initial section of a jet. Under certain conditions the length of a jet before the section S can equal a hundred diameters of the outlet and its breadth can equal value of ten diameters of the outlet.

In the case of a dredging activity simulation, the velocity of a dredger U is comparatively small. For this reason it is possible to suppose that $\sigma_{y'} \sim a$, $\xi_Q=0$ and to offset the point (x_S, y_S) on distances of about $2a$ to $3a$ from the point of the operating device on the direction of the current (here a is the reference size of dredging devices).

In a practical realization of the cloud method, the whole cloud quantity N_c is not very large because a part of clouds can be omitted when their contribution is negligible small due to sedimentation processes. N_c can be approximated roughly by the formula $N_c = \bar{x}/(U\tau_c)$. If $\bar{x}=1\ \ km$, U=0.1 m/sec and τ_c=10 minutes, the hold that $N_c \approx 20$.

2.4 3-D transport diffusion equation

2.4.1 Basic equations

As it was described above, the problem of time-space evolution of pollutants concentrations relatively far from the discharge point is reduced to integration of union of homogeneous equations of transport and turbulent diffusion (2.2.5) with compact distribution of initial pollutants concentrations. Each equation describes the pollution "cloud" (passively transported through the water mass under the currents effect, increases due to turbulent diffusion and possibly deposits on the bottom) evolution. Thus in equation (2.2.5) we could suppose that $u_x = U_x$, $u_y = U_y$ and $u_z + w = W_i$. Also, we should suppose that the diffusivities depend only on the turbulence parameters in the ambient sea water. So, the central point of the problem of pollution spread modeling in the far zone is the standard task of solving for the parabolic equation:

$$\frac{\partial C}{\partial t} + U_x \frac{\partial C}{\partial x} + U_y \frac{\partial C}{\partial y} + W_i \frac{\partial C}{\partial z} = \\ = \frac{\partial}{\partial x}\left(K_x \frac{\partial C}{\partial x} \right) + \frac{\partial}{\partial y}\left(K_y \frac{\partial C}{\partial y} \right) + \frac{\partial}{\partial z}\left(K_z \frac{\partial C}{\partial z} \right), \tag{2.4.1a}$$

with the initial and boundary conditions:

$$t = 0 : C = C^0(x, y, z),$$
$$z = 0 : K_z \frac{\partial C}{\partial z} = u_z C, \qquad (2.4.1b)$$
$$z = H : K_z \frac{\partial C}{\partial z} = (u_z - k) C.$$

Here the initial distribution C^0 of the concentration C could be supposed to be finite ($C^0(x,y,z) \to 0$ as $\sqrt{x^2 + y^2} \to \infty$) and corresponding to the following symmetry conditions: $C^0(x,y,z) = C^0(-x,y,z)$, $C^0(x,y,z) = C^0(x,-y,z)$. We must note again that diffusion factors in equation (2.4.1a) are determined by the turbulent mixing processes and because of this they are affected by the pollution "cloud" dimensions which extend with the course of time (see, for example, [40]).

Below an efficient method of problem (2.4.1) calculation is discussed (see, for example, *Bao-Shi-Shiau at al*. [6]). This method gives a natural way to allow for "cloud" size dependence of diffusion factors and gives a method of initial distribution of C^0 according to the data obtained from the calculation of the stream phase of discharge spread process.

2.4.2 Momentum method of solution of 3-d transport diffusion equation

As a rule, the horizontal scale of zones of interest while modeling of drilling mud and other pollutant discharges is bounded by several hundred meters. That is why we may suppose that U_x, U_y, W_i, K_x, K_y, K_z factors should be constant in this zone and dependent on the time and vertical coordinate z. Let us assume that water H doesn't depend on x and y.

To solve the problem (2.4.1) with compact initial conditions we use the method of moments. Let us denote the concentration moments determined by the expression

$$C_{kl}(z,t) = \int_{-\infty}^{\infty} \int_{-\infty}^{\infty} C(x,y,z,t) x^k y^l dx dy, \qquad (2.4.2)$$

here k, l =0,1,2... is the order of moment.

Using the expression (2.4.2) for the problem (2.4.1) we will get the following recurrent system of equations and edge conditions:

$$\frac{\partial C_{k,l}}{\partial t} - kU_x C_{k-1,l} - lV_y C_{k,l-1} + W_i \frac{\partial C_{k,l}}{\partial z} =$$
$$= k(k-1)K_x C_{k-2,l} + l(l-1)K_y C_{k,l-2} + \frac{\partial}{\partial z}\left(K_z \frac{\partial C_{k,l}}{\partial z} \right), \qquad (2.4.3)$$
$$z = 0 : \; K_z \frac{\partial C_{k,l}}{\partial z} = u_z C_{k,l},$$
$$z = H : \; K_z \frac{\partial C_{k,l}}{\partial z} = (u_z - k) C_{k,l}.$$

The first six moments have an obvious physical meaning. For example, the zero-order moment (k=0, l=0) is similar to the mass density $M(z)$ in the pollution "cloud":

$$M(z,t) = C_{00} = \int_{-\infty}^{+\infty}\int_{-\infty}^{+\infty} C(x,y,z,t)dxdy .$$

Coordinates X_c, Y_c of the "cloud" gravity center are supposed to be represented as relationships of the first moments (k=0, l=1 and k=1, l=0) to the zero moment:

$$X_c(z,t) = C_{10}/C_{00} ,\ Y_c(z,t) = C_{01}/C_{00} .$$

The typical "cloud" dimensions σ_x, σ_y, x and y directed as well as the asymmetry ratio D_{xy} are determined by the following combinations:

$$\sigma_x(z,t) = \sqrt{C_{20}/C_{00} - X_c^2} ,\ \sigma_y(z,t) = \sqrt{C_{02}/C_{00} - Y_c^2} ,$$
$$\sigma_{xy}(z,t) = \sqrt{C_{11}/C_{00} - X_c Y_c} .$$

The six first moments give an opportunity to calculate the Gaussian concentrations distribution in the "cloud":

$$C(x,y,z,t) = \frac{M}{2\pi\sqrt{\sigma_x^2\sigma_y^2 - \sigma_{xy}^4}} \times \exp\left(-\frac{\sigma_x^2\sigma_y^2}{\sigma_x^2\sigma_y^2 - \sigma_{xy}^4}\left[\frac{(x-X_c)^2}{2\sigma_x^2} + \frac{(y-Y_c)^2}{2\sigma_y^2} - \frac{\sigma_{xy}^2(x-X_c)(y-Y_c)}{\sigma_x^2\sigma_y^2}\right]\right). \quad (2.4.4)$$

Then, for the first six moments there seems to be a rather accurate description, because the Gauss distribution of concentrations is experimentally observed upon studying the spread of the different pollutants. Here, we will not go beyond the first six moments.

Let us write the first six moment equations according to the general formulation (2.4.3):

$$\begin{aligned}
&\frac{\partial C_{00}}{\partial t}=\frac{\partial}{\partial z}\left(K_z\frac{\partial C_{00}}{\partial z}\right)-W_i\frac{\partial C_{00}}{\partial z},\\
&\frac{\partial C_{01}}{\partial t}=\frac{\partial}{\partial z}\left(K_z\frac{\partial C_{01}}{\partial z}\right)+U_yC_{00}-W_i\frac{\partial C_{01}}{\partial z},\\
&\frac{\partial C_{10}}{\partial t}=\frac{\partial}{\partial z}\left(K_z\frac{\partial C_{10}}{\partial z}\right)+U_xC_{00}-W_i\frac{\partial C_{10}}{\partial z},\\
&\frac{\partial C_{02}}{\partial t}=\frac{\partial}{\partial z}\left(K_z\frac{\partial C_{02}}{\partial z}\right)+2K_yC_{00}+2U_yC_{01}-W_i\frac{\partial C_{02}}{\partial z},\\
&\frac{\partial C_{11}}{\partial t}=\frac{\partial}{\partial z}\left(K_z\frac{\partial C_{11}}{\partial z}\right)+U_xC_{01}+U_yC_{10}-W_i\frac{\partial C_{11}}{\partial z},\\
&\frac{\partial C_{20}}{\partial t}=\frac{\partial}{\partial z}\left(K_z\frac{\partial C_{20}}{\partial z}\right)+2K_xC_{00}+2U_xC_{10}-W_i\frac{\partial C_{20}}{\partial z}.
\end{aligned}\qquad (2.4.5)$$

The edge conditions of (2.4.3) are specified in (2.4.5). We can get the initial conditions for (2.4.5), if we set the parameters M, X_c, Y_c, σ_x, σ_y and D_{xy} at time t=0 as

$$\begin{aligned}
&C_{00}^0=M,\ C_{10}^0=X_c\cdot M,\ C_{01}^0=Y_c\cdot M,\\
&C_{20}^0=\left(\sigma_x^2+X_c^2\right)\cdot M,\ C_{02}^0=\left(\sigma_y^2+Y_c^2\right)\cdot M,\\
&C_{11}^0=\left(\sigma_{xy}^2+X_cY_c\right)\cdot M.
\end{aligned}\qquad (2.4.6)$$

Diffusivities K_x and K_y are determined by lateral water transport. We obtain locally homogenous and isotropic (laterally) turbulence with Kolmogorov's pulsations spectrum [28] K_x=K_y~$L_c^{4/3}$, where L_c is a typical pollution cloud size. When determining the typical size L_c through the values σ_x, σ_y and D_{xy} (see, for example, [6]), we will obtain the following expression:

$$K_x=K_y=\begin{cases}BL_c^{4/3}, & L_c<L_0\\ BL_0^{4/3}, & L_c\ge L_0\end{cases},\qquad L_c=(\sigma_x^2\sigma_y^2-D_{xy}^2)^{1/4}.$$

Here L_0 is the outer scale of lateral turbulence.

2.4.3 Numerical implementation of pollution cloud diffusion scattering model in 3-D case

The numerical implementation of the system (2.4.5) seems to be rather easy. In the model we use the usual Crank-Nicholson scheme. This scheme constitutes of the following fittings of time and space differential coefficients:

$$\frac{\partial \boldsymbol{F}}{\partial t}=\frac{\boldsymbol{F}_i^{j+1}-\boldsymbol{F}_i^{j}}{\Delta t},\ \frac{\partial \boldsymbol{F}}{\partial z}=\frac{1}{2\Delta z^2}\left[\left(\boldsymbol{F}_{i+1}^{j+1}-2\boldsymbol{F}_i^{j+1}+\boldsymbol{F}_{i-1}^{j+1}\right)+\left(\boldsymbol{F}_{i+1}^{j}-2\boldsymbol{F}_i^{j}+\boldsymbol{F}_{i-1}^{j}\right)\right].$$

In this equation F=(C_{00}, C_{01}, C_{10}, C_{02}, C_{20}, C_{11}), Δt and Δz – are a discrete steps in time and vertical coordinate z, the index marks *i* and *j* relate to the space and time layers, respectively.

The obtained linear system of equations for unknown mesh functions could be efficiently solved by the sweep method on the upper time layer.

2.4.4 Generation of pollution clouds in the nearest zone in 3-d case

According to the above concept for the simulation of time-space evolution of any of the pollutant cuts in the far zone the stream could be divided into ordinary segments with length *ds*. Each of these segments could be considered as a point pollution source, situated at the point $r_j=(x_j, y_j, z_j)$ of the stream axis. We should also enter two additional sources, situated in the stream beginning (the model of matter transport into upper plume) and the stream end. We could determine for each continuous source (as a result of the evaluation of the stream phase of discharge), three main parameters:

1) mass consumption Q [kg/s];
2) pollutant concentration C_j [kg/м3] in the stream section, which corresponds to point r_j;
3) typical vertical dimension of the stream L_z at this point.

The total time of operation is divided into time intervals of length Δt. During these intervals, the nearest zone generates a separate pollution "cloud". Then all these "clouds" spread in water mass corresponding to the laws described below. S separate pollutant concentration at a given space point r and given time t could be described as the concentrations summation of the discussed pollutant by all "clouds" which are positioned at a given time t at the point *r*. The initial parameters of each pollution "cloud" generated by the end of the time interval Δt, i.e. the initial conditions for equations (2.4.5) in the model are calculated by the following algorithm. We define a rather small mass value m (concentrated in the "cloud") of the discussed type pollutant. The time interval Δt is calculated by the formula $\Delta t=m/Q$. We define the "cloud" size (vertically) equal to L_z, and the other initial parameters are as follows:

$$M = \frac{m}{L_z},\ \sigma_x = \sigma_y = \sqrt{\frac{M}{2\pi C_j}},\ \sigma_{xy} = 0,$$

$$X_c = x_j + U_x \Delta t, \qquad Y_c = y_j + U_y \Delta t, \qquad Z_c = z_j + W_i \Delta t.$$

Here Z_c is the vertical coordinate of the "cloud" center. At $z>Z_c+L_z/2$ and $z<Z_c-L_z/2$ the moments $C_{ij}^0=0$. If we get in our calculations that $Z_c+L_z/2>H$, the "cloud" part in the model which corresponds to the coordinate $H<z< Z_c+L_z/2$ will be considered as sediment one.

2.4.5 Some results of 3-d model

In Article [I], some results are given for environment conditions and source intensity variable in time consistent with the scenario of technological operations. Below the example of calculations on the 3-d model with a constant source intensity and non-variable current velocity is given.

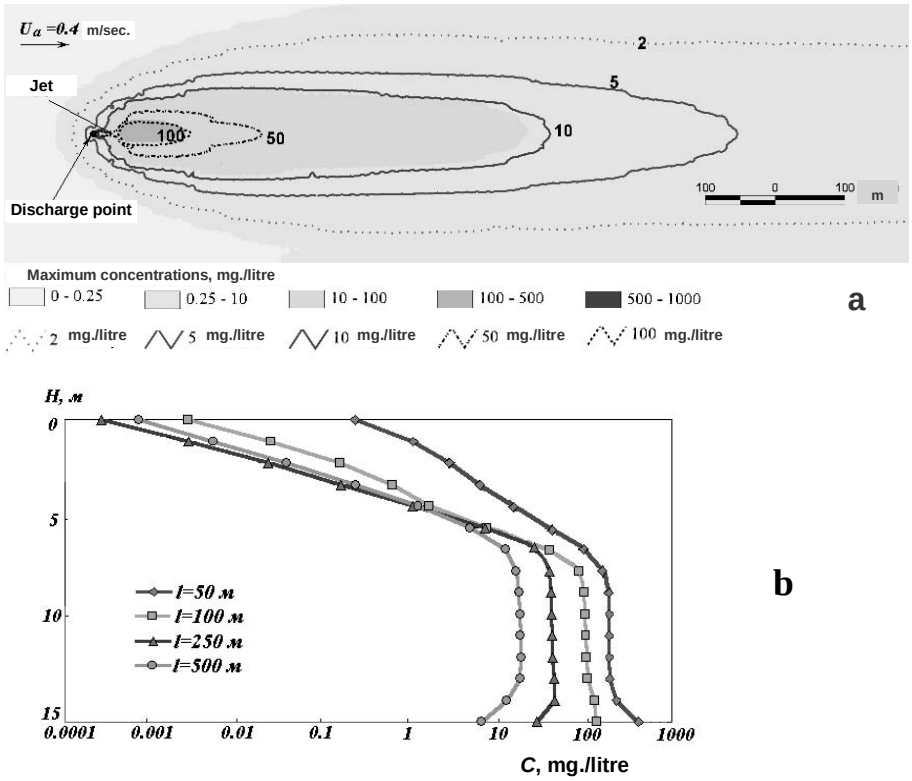

FIGURE 2.4.1: Distribution of concentrations of SS from a stationary source (a) concentration averaged on depth, plane view, (b) vertical section at different distances of the source.

2.5 Conclusions

The considered models allow us to build effective methods of calculations of CS dispersion in water environment. The method takes into account the change of diffusivities with the growth of contaminated region dimensions. The method avoids the drawback inherent in methods of finite differences and discrete particles, which don't necessarily account the changing diffusivities with dimension growth of the contaminated region.

3 HYDRODYNAMIC PROCESSES SIMULATIONS

3.1 The basic equations definition

A conventional system of the three-dimensional equations of geophysical hydrodynamics is used to describe the state parameters of the water object. This system is derived with the assumption of a permanent-type density and f - plane, when forces arisen due to the Earth gyration are expressed in a form with the fixed value of the Coriolis parameter ($f \approx 10^{-4}[s^{-1}]$). The basic designations are shown in Figure 3.1.1.

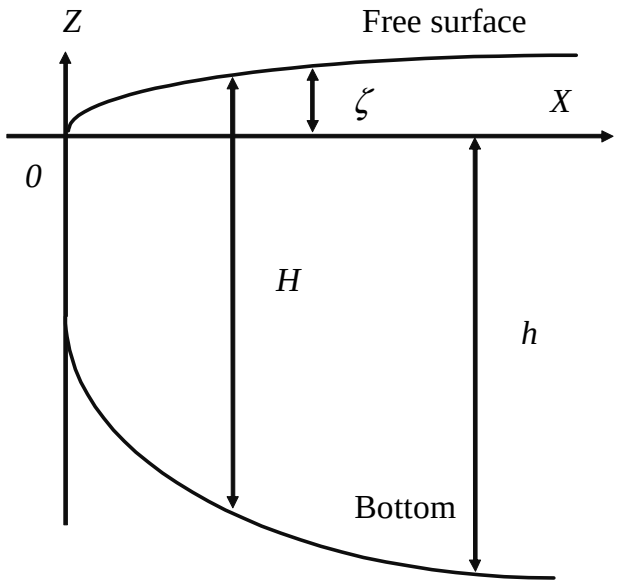

FIGURE 3.1.1: Main designations.

The system has the following form:

$$\frac{\partial u}{\partial x}+\frac{\partial v}{\partial y}+\frac{\partial w}{\partial z}=0\,, \tag{3.1.1}$$

$$\begin{aligned}&\frac{\partial u}{\partial t}+\frac{\partial}{\partial x}u^2+\frac{\partial}{\partial y}vu+\frac{\partial}{\partial z}wu-fv\\&\quad=-\frac{1}{\rho_0}\frac{\partial P}{\partial x}+N_h\left(\frac{\partial^2 u}{\partial x^2}+\frac{\partial^2 u}{\partial y^2}\right)+\frac{\partial}{\partial z}\left(N_z\frac{\partial u}{\partial z}\right),\end{aligned} \tag{3.1.2}$$

$$\begin{aligned}&\frac{\partial v}{\partial t}+\frac{\partial}{\partial x}v^2+\frac{\partial}{\partial y}v^2+\frac{\partial}{\partial z}wv+fu\\&\quad=-\frac{1}{\rho_0}\frac{\partial P}{\partial y}+N_h\left(\frac{\partial^2 v}{\partial x^2}+\frac{\partial^2 v}{\partial y^2}\right)+\frac{\partial}{\partial z}\left(N_z\frac{\partial v}{\partial z}\right),\end{aligned} \tag{3.1.3}$$

$$0=-\frac{1}{\rho_0}\frac{\partial P}{\partial z}+g\,. \tag{3.1.4}$$

The boundary conditions on the surface and the bottom of the pool are in the following form:

$$N_z\frac{\partial u}{\partial z}=\tau_x^0,\;\; N_z\frac{\partial v}{\partial z}=\tau_y^0\;\;,$$

$$\tau=\rho_a/\rho_w\, C_d\cdot {V_{10}}^2,\;\; \tau_x^0=\tau\sin(\varphi),\;\; \tau_y^0=\tau\cos(\varphi)\,, \tag{3.1.5}$$

$$C_d=\begin{cases}1.1\cdot 10^{-3},\; V_{10}<6\text{ m/s}\\ \left(0.72+0.063\cdot|V_{10}|\right)\cdot 10^{-3},\; V_{10}>6\text{m/s}'\end{cases}$$

$$N_z\frac{\partial u}{\partial z}=\tau_{0x}, N_z\frac{\partial v}{\partial z}=\tau_{0y}, \tau_{0x}=\alpha|\vec{u}|u, \tau_{0y}=\alpha|\vec{u}|v. \tag{3.1.6}$$

The expression for pressure is used in hydrostatic approximation [16]:

$$\frac{1}{\rho_0}\frac{\partial P}{\partial x}=\frac{1}{\rho_0}\frac{\partial}{\partial x}\int_z^\zeta(\rho_w\cdot g)dz\approx g\cdot\frac{\partial\zeta}{\partial x}+\frac{g}{\rho_0}\int_z^\zeta\frac{\partial}{\partial x}(\rho_w)\,dz \tag{3.1.7}$$

All the assumptions above result in the following system:

$$\frac{\partial u}{\partial x}+\frac{\partial v}{\partial y}+\frac{\partial w}{\partial z}=0\,, \tag{3.1.8}$$

$$\begin{aligned}&\frac{\partial u}{\partial t}+\frac{\partial}{\partial x}u^2+\frac{\partial}{\partial y}vu+\frac{\partial}{\partial z}wu-fv\\&\quad=-g\frac{\partial\varsigma}{\partial x}+N_h\left(\frac{\partial^2 u}{\partial x^2}+\frac{\partial^2 u}{\partial y^2}\right)+\frac{\partial}{\partial z}\left(N_z\frac{\partial u}{\partial z}\right),\end{aligned} \tag{3.1.9}$$

$$\frac{\partial v}{\partial t}+\frac{\partial}{\partial x}v^2+\frac{\partial}{\partial y}v^2+\frac{\partial}{\partial z}wv+fu$$
$$=-g\frac{\partial \varsigma}{\partial y}+N_h\left(\frac{\partial^2 v}{\partial x^2}+\frac{\partial^2 v}{\partial y^2}\right)+\frac{\partial}{\partial z}\left(N_z\frac{\partial v}{\partial z}\right). \qquad (3.1.10)$$

Kinematic relations on a surface and bottom of a pool are the additional conditions, which have the following form:

$$\frac{\partial \zeta}{\partial t}+u\frac{\partial \zeta}{\partial x}+v\frac{\partial \zeta}{\partial y}=w,\ u\frac{\partial h}{\partial x}+v\frac{\partial h}{\partial y}=w.$$

Here is a brief derivation of the kinematic relation on the surface:

$$R(x,y,z)=0,\ R:\ z-\varsigma(t,x,y)=0,\ \frac{d}{dt}\left[z-\varsigma(t,x,y)\right]=0,$$
$$\frac{dz}{dt}-\frac{\partial \varsigma}{\partial t}-\frac{\partial \varsigma}{\partial x}\frac{dx}{dt}-\frac{\partial \varsigma}{\partial y}\frac{dy}{dt}=0,\ w=\frac{\partial \varsigma}{\partial t}+\frac{\partial \varsigma}{\partial x}u+\frac{\partial \varsigma}{\partial y}v.$$

The system (3.1.8)-(3.1.10) with cinematic conditions is named the "system with free surface" in contrast with the system with "rigid lid" [11], where surface gravity waves are excluded. The sigma coordinate system is probably a necessary attribute in dealing with significant topographical variability. Transformation of the coordinates consist of the following set of relations (a tilde denotes initial variables):

$$t=\tilde{t},\ x=\tilde{x},\ y=\tilde{y},\ \sigma=f(\tilde{t},\tilde{x},\tilde{y},z),$$
$$\sigma=\frac{z+h}{\varsigma+h},\ z=(\varsigma+h)\sigma-h\equiv H\sigma-h, \qquad (3.1.11)$$
$$\sigma\in\{0,\ 1\},\ z\in\{-h,\ \varsigma\},\ J=\frac{\partial z}{\partial \sigma}=\varsigma+h\equiv H.$$

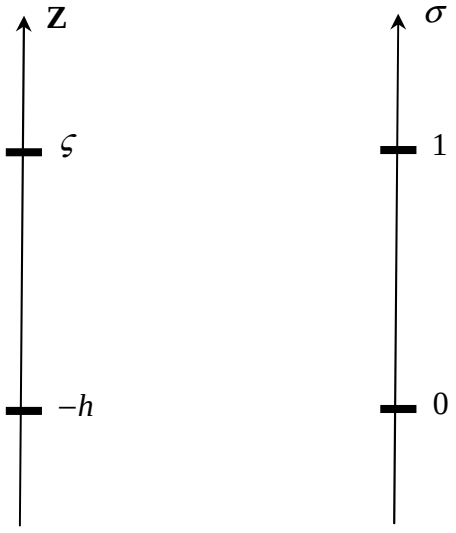

FIGURE 3.1.2: Correspondence of vertical coordinates (3.1.11).

In the sigma coordinate system the equations (3.1.1)-(3.1.3) take the following form (tilde is omitted and derivatives by x, y are taken under the constant σ):

$$\frac{\partial J}{\partial t}+\frac{\partial (uJ)}{\partial x}+\frac{\partial (vJ)}{\partial y}+\frac{\partial}{\partial \sigma}\left(w-\frac{dz}{dt}-u\frac{\partial (z)}{\partial x}-v\frac{\partial (z)}{\partial y}\right)=0, \tag{3.1.12}$$

$$\begin{aligned}&\frac{\partial (Ju)}{\partial t}+\frac{\partial (uJu)}{\partial x}+\frac{\partial (vJu)}{\partial y}+\frac{\partial}{\partial \sigma}\left[u\left(w-\frac{dz}{dt}-u\frac{\partial z}{\partial x}-v\frac{\partial z}{\partial y}\right)\right]\\ &=\left[-\frac{\partial}{\partial x}\left(\frac{P}{\rho_0}J\right)+\frac{\partial}{\partial \sigma}\left(\frac{P}{\rho_0}\frac{\partial z}{\partial x}\right)\right]+Jfu\end{aligned} \tag{3.1.13}$$

$$+\left[\frac{\partial (JQ_{ux})}{\partial x}+\frac{\partial (JQ_{uy})}{\partial y}+\frac{\partial}{\partial \sigma}\left(Q_{uz}-\frac{dz}{dx}Q_{ux}-\frac{\partial z}{\partial y}Q_{uy}\right)\right],$$

$$\begin{aligned}&\frac{\partial (Jv)}{\partial t}+\frac{\partial (uJv)}{\partial x}+\frac{\partial (vJv)}{\partial y}+\frac{\partial}{\partial \sigma}\left[v\left(w-\frac{dz}{dt}-u\frac{\partial (z)}{\partial x}-v\frac{\partial (z)}{\partial y}\right)\right]\\ &=\left[-\frac{\partial}{\partial y}\left(\frac{P}{\rho_0}J\right)+\frac{\partial}{\partial \sigma}\left(\frac{P}{\rho_0}\frac{\partial z}{\partial y}\right)\right]+Jfu\end{aligned} \tag{3.1.14}$$

$$+\left[\frac{\partial (JQ_{vx})}{\partial x}+\frac{\partial (JQ_{vy})}{\partial y}+\frac{\partial}{\partial \sigma}\left(Q_{vz}-\frac{dz}{dx}Q_{vx}-\frac{\partial z}{\partial y}Q_{vy}\right)\right].$$

Here Q denotes viscous terms. There is the ability to average the equations (3.1.12)–(3.1.14) (i.e. by means of integration from top to bottom of the pool $\overline{f}=\int_0^1 J\cdot f\ d\sigma$). Introducing

$$H=\varsigma+h,\ U=\int_{-h}^{\varsigma} u dz,\ V=\int_{-h}^{\varsigma} v dz, \tag{3.1.15}$$

and taking into account kinematic relations we get the system of equations:

$$\frac{\partial \zeta}{\partial t}+\frac{\partial U}{\partial x}+\frac{\partial V}{\partial y}=0,$$

$$\begin{aligned}&\frac{\partial U}{\partial t}+\frac{\partial \overline{u^2}}{\partial x}+\frac{\partial \overline{uv}}{\partial y}-fV\\ &=\left[-\frac{\partial}{\partial x}\left(\frac{gH^2}{2}\right)+gH\frac{\partial h}{\partial x}\right]+\left(\frac{\partial}{\partial x}\overline{Q_{ux}}+\frac{\partial}{\partial y}\overline{Q_{uy}}\right)+\left(\widehat{\tau_x^0}-\widehat{\tau_{0x}}\right),\end{aligned} \tag{3.1.16}$$

$$\begin{aligned}&\frac{\partial V}{\partial t}+\frac{\partial \overline{uv}}{\partial x}+\frac{\partial \overline{v^2}}{\partial y}+fU\\ &=\left[-\frac{\partial}{\partial y}\left(\frac{gH^2}{2}\right)+gH\frac{\partial h}{\partial y}\right]+\left(\frac{\partial}{\partial x}\overline{Q_{vx}}+\frac{\partial}{\partial y}\overline{Q_{vy}}\right)+\left(\widehat{\tau_y^0}-\widehat{\tau_{0y}}\right).\end{aligned}$$

It should be mentioned that while deducing (3.1.16) we didn't propose any

additional assumptions. Introducing average variables, $u_x = \frac{1}{H}\int_{-h}^{\zeta} u dz,\ u_y = \frac{1}{H}\int_{-h}^{\zeta} v dz$, dispersion and other necessary guesses for "closure" of system we obtain from the (3.1.16) the known equations of shallow water (we return to old notations for average):

$$\frac{\partial H}{\partial t} + \frac{\partial (Hu)}{\partial x} + \frac{\partial (Hv)}{\partial y} = 0,$$

$$\frac{\partial (Hu)}{\partial t} + \frac{\partial (Hu^2)}{\partial x} + \frac{\partial (Huv)}{\partial y} - fHv$$

$$= -\frac{\partial \left(gH^2/2 \right)}{\partial x} + gH\frac{\partial h}{\partial x} + K\left\{ \frac{\partial^2 (Hu)}{\partial x^2} + \frac{\partial^2 (Hu)}{\partial y^2} \right\} + \left(\tau_x^0 - \tau_{0x} \right),$$

$$\frac{\partial (Hv)}{\partial t} + \frac{\partial (Huv)}{\partial x} + \frac{\partial (Hv^2)}{\partial y} + fHu$$

$$= -\frac{\partial \left(gH^2/2 \right)}{\partial y} + gH\frac{\partial h}{\partial y} + K\left\{ \frac{\partial^2 (Hv)}{\partial x^2} + \frac{\partial^2 (Hv)}{\partial y^2} \right\} + \left(\tau_y^0 - \tau_{0y} \right).$$

In the divergent form the system takes the following form:

$$\frac{\partial H}{\partial t} + \frac{\partial U}{\partial x} + \frac{\partial V}{\partial y} = 0,$$

$$\frac{\partial (Hu)}{\partial t} + \frac{\partial \left(U^2/H + gH^2/2 \right)}{\partial x} + \frac{\partial \left(UV/H \right)}{\partial y}$$

$$= +fV + gH\frac{\partial h}{\partial x} + K\left\{ \frac{\partial^2 U}{\partial x^2} + \frac{\partial^2 U}{\partial y^2} \right\} + \left(\tau_x^0 - \tau_{0x} \right), \qquad (3.1.17)$$

$$\frac{\partial (Hv)}{\partial t} + \frac{\partial \left(UV/H \right)}{\partial x} + \frac{\partial \left(V^2/H + gH^2/2 \right)}{\partial y}$$

$$= -fU + gH\frac{\partial h}{\partial y} + K\left\{ \frac{\partial^2 V}{\partial x^2} + \frac{\partial^2 V}{\partial y^2} \right\} + \left(\tau_y^0 - \tau_{0y} \right).$$

In the vector form (3.1.17) is

$$\frac{\partial \vec{U}}{\partial t} + \frac{\partial \vec{F}}{\partial x} + \frac{\partial \vec{G}}{\partial y} = \vec{R},$$

where

$$\vec{U} = \begin{Bmatrix} H \\ U \\ V \end{Bmatrix},\ \vec{F} = \begin{Bmatrix} U \\ U^2/H + 0.5gH^2 \\ UV/H \end{Bmatrix},\ \vec{G} = \begin{Bmatrix} V \\ UV/H \\ V^2/H + 0.5gH^2 \end{Bmatrix}.$$

The quasilinear gradient form is useful for investigation:

$$\frac{\partial \vec{U}}{\partial t}+\frac{\partial \vec{F}}{\partial \vec{U}}\frac{\partial \vec{U}}{\partial x}+\frac{\partial \vec{G}}{\partial \vec{U}}\frac{\partial \vec{U}}{\partial y}=\vec{R},\ \frac{\partial \vec{U}}{\partial t}+A\frac{\partial \vec{U}}{\partial x}+B\frac{\partial \vec{U}}{\partial y}=\vec{R},\ A\equiv\frac{\partial \vec{F}}{\partial \vec{U}},\ \ B\equiv\frac{\partial \vec{G}}{\partial \vec{U}}, \qquad (3.1.18)$$

where $A\equiv\frac{\partial \vec{F}}{\partial \vec{U}}=\begin{pmatrix}0 & 1 & 0\\ c^2-u^2 & 2u & 0\\ -uv & v & u\end{pmatrix}$, $B\equiv\frac{\partial \vec{G}}{\partial \vec{U}}=\begin{pmatrix}0 & 0 & 1\\ -uv & v & u\\ c^2-v^2 & 0 & 2v\end{pmatrix}$,

$c=\sqrt{gh},\ u=\frac{U}{H},\ v=\frac{V}{H}$.

3.2 Boundary conditions on the lateral boundary

3.2.1 Boundary conditions on the solid lateral boundary

On a solid lateral surface in a boundary layer in the zone of a logarithmic velocity profile we use the following conditions:

$$u_n=0,\ \nu_T\frac{\partial u_\tau}{\partial n}=\mathrm{v}_*^2,\ \mathrm{v}_*=\frac{\kappa\ u_\tau}{\ln\left(30n/h_w\right)}, \qquad (3.2.1)$$

here u_n and u_τ are the normal and tangential component velocities on the boundary of the simulated region, n is the distance from a considered point up to the boundary, counting in the direction of an interior normal line, v_* is the dynamic velocity, κ=0.4 is the Karman constant and h_w is the equivalent height of surface roughness. These formulas are used for a statement of edge requirements in the boundary meshes of a finite difference grid near the solid boundary.

3.2.2 Boundary conditions on the open lateral boundary

Specification of boundary conditions on the open boundary is realized in two stages. First of all, boundary conditions for the equations of shallow water are to be considered (3.1.17). After that it is necessary to make residual definitions for the three-dimensional equations (3.1.8) - (3.1.10) (see [44] and [56]).

Such stage-by-stage open boundary condition introduction for the system (3.1.8) - (3.1.10) is necessary as a result of the decision variable dissymmetry ($\varsigma(t,x,y)$, $u(t,x,y,z)$, $v(t,x,y,z)$ and $w(t,x,y,z)$). The group of variables $H=\varsigma+h$, $U=\int_{-h}^{\varsigma}udz$ and $V=\int_{-h}^{\varsigma}vdz$ form a hyperbolic part of a problem relating to gravity waves. The group $u(t,x,y,z)$, $v(t,x,y,z)$ is attached to the first one, and finally $w(t,x,y,z)$ is separately included into to the system, it can be found from the the equation of continuity and the kinematic condition.

For the boundary condition definition for the variables $\varsigma(t,x,y)$, $u(t,x,y,z)$, $v(t,x,y,z)$ first of all it is necessary to define the boundary conditions for *H, U, V*. For this purpose the eigenvalues problem of the matrix A are solved (see (3.1.18)):

$(l,m,n)(A-\lambda E)=0$,
where E is the unitary matrix.

Hence we find the set of eigenvalues and corresponding eigenvectors:

$$\lambda_1 = u,\ (l_1,m_1,n_1)=(\frac{v}{H},0,-\frac{1}{H}),$$
$$\lambda_2 = u+c,\ (l_2,m_2,n_2)=(\frac{c-u}{H},\frac{1}{H},0),$$
$$\lambda_3 = u-c,\ (l_3,m_3,n_3)=(\frac{c+u}{H},-\frac{1}{H},0).$$

The following relations are obtained via multiplication of the equation (3.1.17) by a eigenvector of the matrix A:

$$(l,m,n)\frac{\partial\vec{U}}{\partial t}+(l,m,n)A\frac{\partial\vec{U}}{\partial x}+(l,m,n)B\frac{\partial\vec{U}}{\partial y}=(l,m,n)R,$$
$$(l,m,n)\frac{\partial\vec{U}}{\partial t}+(\lambda l,\lambda m,\lambda n)\frac{\partial\vec{U}}{\partial x}+(l_B,m_B,n_B)\frac{\partial\vec{U}}{\partial y}=\tilde{R},$$
$$l\frac{\partial H}{\partial t}+m\frac{\partial U}{\partial t}+n\frac{\partial V}{\partial t}+\lambda\left(l\frac{\partial H}{\partial x}+m\frac{\partial U}{\partial x}+n\frac{\partial V}{\partial x}\right)+(l_B,m_B,n_B)\frac{\partial\vec{U}}{\partial y}=\tilde{R}.$$

It should be mentioned that (l_B,m_B,n_B) are not eigenvectors of the matrix B and are only the product of the multiplication of B and the eigenvector of the matrix A. Introducing Riemann's invariants $\Phi(H,U,V)$ we obtain:

$$d\Phi=\frac{\partial\Phi}{\partial H}dH+\frac{\partial\Phi}{\partial U}dU+\frac{\partial\Phi}{\partial V}dV.$$

The functional form of these invariants is resolved from relations:
$\frac{\partial\Phi}{\partial H}=l;\frac{\partial\Phi}{\partial U}=m;\frac{\partial\Phi}{\partial V}=n.$
The eigenvectors are defined by the following equations:

$$\frac{v}{H}\frac{\partial H}{\partial t}-\frac{1}{H}\frac{\partial V}{\partial t}+\lambda_1\left(\frac{v}{H}\frac{\partial H}{\partial x}-\frac{1}{H}\frac{\partial V}{\partial x}\right)+(l_B,m_B,n_B)\frac{\partial\vec{U}}{\partial y}=\tilde{R},$$
$$\frac{c-u}{H}\frac{\partial H}{\partial t}+\frac{1}{H}\frac{\partial U}{\partial t}+\lambda_2\left(\frac{c-u}{H}\frac{\partial H}{\partial x}+\frac{1}{H}\frac{\partial U}{\partial x}\right)+(l_B,m_B,n_B)\frac{\partial\vec{U}}{\partial y}=\tilde{R}$$

and

$$\frac{c+u}{H}\frac{\partial H}{\partial t}-\frac{1}{H}\frac{\partial U}{\partial t}+\lambda_3\left(\frac{c+u}{H}\frac{\partial H}{\partial x}-\frac{1}{H}\frac{\partial U}{\partial x}\right)+(l_B,m_B,n_B)\frac{\partial \vec{U}}{\partial y}=\tilde{R}.$$

Three Riemann's invariants are determined:

$$\Phi_1=-\frac{V}{H}\equiv -v,\quad \frac{\partial \Phi_1}{\partial H}=\frac{v}{H},\quad \frac{\partial \Phi_1}{\partial U}=0,\quad \frac{\partial \Phi_1}{\partial V}=-\frac{1}{H},$$

$$\Phi_2=u+2c,\quad \frac{\partial \Phi_2}{\partial H}=\frac{c-u}{H},\quad \frac{\partial \Phi_2}{\partial U}=\frac{1}{H},$$

$$\Phi_3=u-2c,\quad \frac{\partial \Phi_3}{\partial H}=\frac{c+u}{H},\quad \frac{\partial \Phi_2}{\partial U}=-\frac{1}{H}.$$

Thus, on the open boundary, through which a fluid flows in, two characteristic curves $\lambda_1=u$, $\lambda_2=u+c$ enter the considered area and one $\lambda_3=u-c$ goes out. In the case the outflow from the area one characteristic curve $\lambda_2=u+c$ goes into the region and the pair $\lambda_1=u$, $\lambda_3=u-c$ go outside it. For systems like (3.1.17) but without viscosity such structure of hyperbolic equations would set the amount and the type of boundary conditions, but the presence of viscosity suggests the following form of boundary conditions [30]. Namely to u_n, u_τ and H are assigned values to conserve the two Riemann's invariants, and the third Riemann's invariant is extrapolated to the boundary inside region:

$$u_\tau=u_{\tau 0}, \tag{3.2.2}$$

$$u_n+2\sqrt{gH}=u_{n0}+2\sqrt{gH_0}, \tag{3.2.3}$$

$$\frac{\partial}{\partial n}\left(u_n-2\sqrt{gH}\right)=0. \tag{3.2.4}$$

On that part of the exterior boundary, through which fluid outflows, for the depth H one requirement of radiation is superimposed and for the remaining variables the so-called weak requirements are specified:

$$u_n+2\sqrt{gH}=u_{n0}+2\sqrt{gh},\ \frac{\partial^2 f}{\partial l^2}=0,\quad f=u_n,u_\tau, \tag{3.2.5}$$

here $\partial^2/\partial l^2$ is the second derivative in direction of undisturbed flow.

It should be noted that the condition (3.2.3) might be represented in another form [51]:

$$u_n-u_{n0}=-2(\sqrt{gH_0}-\sqrt{gH})=$$

$$=-2\frac{(\sqrt{gH_0}-\sqrt{gH})\cdot(\sqrt{gH_0}+\sqrt{gH})}{(\sqrt{gH_0}+\sqrt{gH})}=$$

$$=-2\frac{(gH_0-gH)}{(\sqrt{gH_0}+\sqrt{gH})}\approx\frac{c}{H}(\varsigma-\varsigma_0)$$

Finally it is possible to write [41], [42], [46]:

$$u_n - u_{n0} = \frac{c}{H}(\varsigma - \varsigma_0). \qquad (3.2.6)$$

After requirements (3.2.2) - (3.2.5) are defined, the hyperbolic part of the problem (connected with propagation of surface gravity waves) is taken into account. On the second step vertical velocity profiles are specified:

$$u = u_0(z),\ v = v_0(z). \qquad (3.2.7)$$

Adduction of the equations of shallow water to the characteristic form is necessary on the one hand for the exact definition of the boundary condition for shallow water problem and on the other hand it is required for specifying boundary conditions for a tree-dimensional system. In this case (3.2.2) – (3.2.5) it is necessary to specify the velocity profiles but, be compatible with the shallow water formulation, i.e. $U = \int_{-h}^{\varsigma} u dz,\ V = \int_{-h}^{\varsigma} v dz$.

Thus it should be emphasized that the specification of u and v on the open boundary is not arbitrary and corresponds with total flows.

3.2.3 Numerical solution method

For approximation, a spatial grid is introduced: $x_i, y_j, z_k,\ x_i = i \cdot \Delta x,\ i = 0,...,N_x,$

$y_j = j \cdot \Delta y,\ j = 0,...,N_y,\ z_0 = \varsigma,\ z_k = z_0 + \sum_{k=1}^{N_z} \Delta z_k,\ k = 0,...,N_z.$

The horizontal steps are uniform, while the vertical steps are variable. The upper layer $\Delta z_1 = z_0 - z_1 \equiv \varsigma - z_1$ is varied in time in contrast to deeper layers, for this reason not the same approximation is used for layers. The staggered grid arrangement for the problem [2], [3] is depicted in Figure 3.2.1 and in Figure 3.2.2

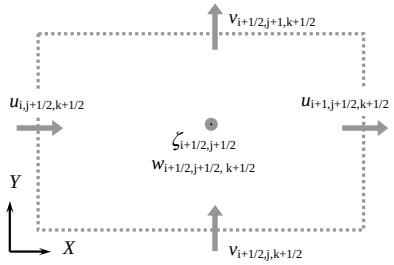

FIGURE 3.2.1: The grid nodes location in horizontal direction.

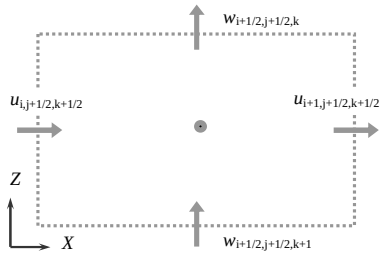

FIGURE 3.2.2: The grid nodes location in vertical direction.

First we shall the consider approximation of hydrodynamic equations in time. For this purpose we use the two-layer semi-implicit scheme, i.e. we consider variables on two time layers n and $n+1$. The stability of this scheme was investigated in [22].

$$\frac{u^{n+1}-u^n}{\Delta t} = -g\frac{\partial\,\varsigma^n}{\partial x} + \frac{\partial}{\partial z}\left(N_z\frac{\partial u^{n+1}}{\partial z}\right) + Au^n, \tag{3.2.8}$$

$$\frac{v^{n+1}-v^n}{\Delta t} = -g\frac{\partial\,\varsigma^n}{\partial y} + \frac{\partial}{\partial z}\left(N_z\frac{\partial v^{n+1}}{\partial z}\right) + Av^n,$$

$$\frac{\zeta^{n+1}-\varsigma^n}{\Delta t} + \frac{\partial U^n}{\partial x} + \frac{\partial V^n}{\partial y} = 0, \tag{3.2.9}$$

$$H^n = \varsigma^n + h,$$

$$U^n = \sum_{k=0}^{k=N_z} u^n_{i,j+1/2,k+1/2}\left(z_k - z_{k+1}\right),\ V^n = \sum_{k=0}^{k=N_z} v^n_{i+1/2,j,k+1/2}\left(z_k - z_{k+1}\right). \tag{3.2.10}$$

A three-point template is used to approximate the vertical viscosity operator.

$$\frac{\partial}{\partial z}\left(N_z\frac{\partial u}{\partial z}\right) \approx \frac{\tau_{k+1}-\tau_k}{\Delta z_k},\ \tau_k = \frac{u_{k+1/2}-u_{k-1/2}}{0.5\left(\Delta z_k + \Delta z_{k-1}\right)}, \tag{3.2.11}$$

where $\tau_0 = \tau_x^0,\ \ \tau_{N_z} = \tau_{0x}$.

Boundary conditions on a surface and bottom of a pool are taken into account in approximation of vertical viscosity in the upper and bottom mesh layers. The approximation of advective terms is illustrated by the example of the equation for a component u:

$$\begin{aligned}&\frac{\partial}{\partial x}u^2 + \frac{\partial}{\partial y}vu + \frac{\partial}{\partial z}wu - fv\\ &\approx \frac{\overline{u}_{i+1/2}\tilde{u}_{i+1/2} - \overline{u}_{i-1/2}\tilde{u}_{i-1/2}}{\Delta x} + \frac{\overline{v}_{i,j+1}\tilde{u}_{i,j+1} - \overline{v}_{i,j-1}\tilde{u}_{i,j-1}}{\Delta y}\\ &+ \frac{\overline{w}_{i,k}\tilde{u}_{i,k} - \overline{w}_{i,k+1}\tilde{u}_{i,k+1}}{\Delta z} - f\frac{v_{i+1/2,j+1} + v_{i+1/2,j} + v_{i-1/2,j+1} + v_{i-1/2,j}}{4}.\end{aligned} \tag{3.2.12}$$

In this expression the variables with "dash" are taken by the rule of "half-sums", and the variables with "tilde" are given in form of the “upwind difference”, for example:

$$\bar{u}_{i+1/2} = \frac{u_{i+1} + u_i}{2},\ \tilde{u}_{i+1/2} = \begin{cases} u_i, & \mathrm{u_i} \geq 0 \\ u_{i+1}, & \mathrm{u_i} < 0 \end{cases}.$$

It must be noted that this difference scheme satisfies the mass conservation law and accounting for the possibility of simulation aria to vary in time [34]. The approximation of open boundary conditions is illustrated by the example of cells on the "east" boundary where fluid through flows inside (Figure 3.2.3).

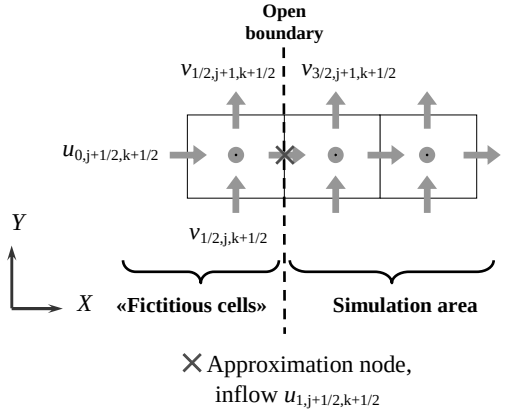

FIGURE 3.2.3: Approximation of open boundary conditions (“east” boundary).

Equation (3.2.2) is approximated in node 1, j in the following form:

$$\frac{v_{1/2,j} + v_{3/2,j}}{2} = v_\tau . \qquad (3.2.13)$$

Equations (3.2.3) – (3.2.5) are approximated in node $1, j+1/2$ in the following form:

$$u_1 + \sqrt{g(\zeta_{1/2} + h_{1/2})} + \sqrt{g(\zeta_{3/2} + h_{3/2})} = u_{n0} + 2\sqrt{gH_0}\,, \qquad (3.2.14)$$

$$\frac{\left(u_2 + \left(g(\zeta_{5/2} + h_{5/2})\right)^{1/2} + \left(g(\zeta_{3/2} + h_{3/2})\right)^{1/2}\right) - \left(u_1 + \left(g(\zeta_{3/2} + h_{3/2})\right)^{1/2} + \left(g(\zeta_{1/2} + h_{1/2})\right)^{1/2}\right)}{\Delta x} = 0. \qquad (3.2.15)$$

It should be mentioned that the sought quantities are u_1 and $\zeta_{1/2}$.

3.2.4 Results of simulations and conclusions

The surveyed equations and methods of the solution have been applied to several types of problems: the problem of simulating the tidal processes in Baidara Bay (Kara Sea) [II], the problem of a flow around an object located in the Northern part of the Caspian Sea [III] and to the problem of three-

dimensional circulation in Jyvasjarvi Lake [V]. For the first two problems, the methods described in sections 3.1 and 3.2 have been applied and for the third problem the widely used Princeton Ocean Model has been used [35]. All approaches are unified by the problem of lateral boundary conditions that are analyzed in the present work. The specific results obtained in modeling calculations are expounded in [II], [III] and [V].

4 HYDRODYNAMIC MODELING AND INFORMATION SYSTEMS

Dispersion models are intended to simulate the fate of neutrally buoyant constituents (often called scalars), such as coliform organisms or ammonium-nitrogen, positively buoyant scalars such as floatable materials, negatively buoyant scalars such as suspended materials, and biota such as plankton or fish, and to provide input to seabed models that simulate the fate of settled materials. Even though dispersion models have been around in one form or another for more than 30 years, and three-dimensional models for more than a decade, the need for improvements in such models still drives the development of better models. In general, it should always be remembered that models are simplifications of reality that allow us to make predictions that hopefully have beneficial uses. However, it should not be assumed that just because a model appears to "work", that the results are representative of the real world. Proof that a model works as desired is really application (or site) specific, and a model's predictive ability should be verified as often as possible, and under different conditions. Potential Circulation and Dispersion modeling components are conceptualized in Figure 4.1.

The Figure 4.1. consists of four parts:

1. Data Requirements: Information required to run the model.
2. Modeling components: The various models needed to make the desired predictions over the time and spatial scales of concern.
3. Output: The predicted results generated by the models, which may not be in a readily understandable form.
4. Post processing: The use of state-of-the-art GIS and visualization tools used to display complex three-dimensional modeling results.

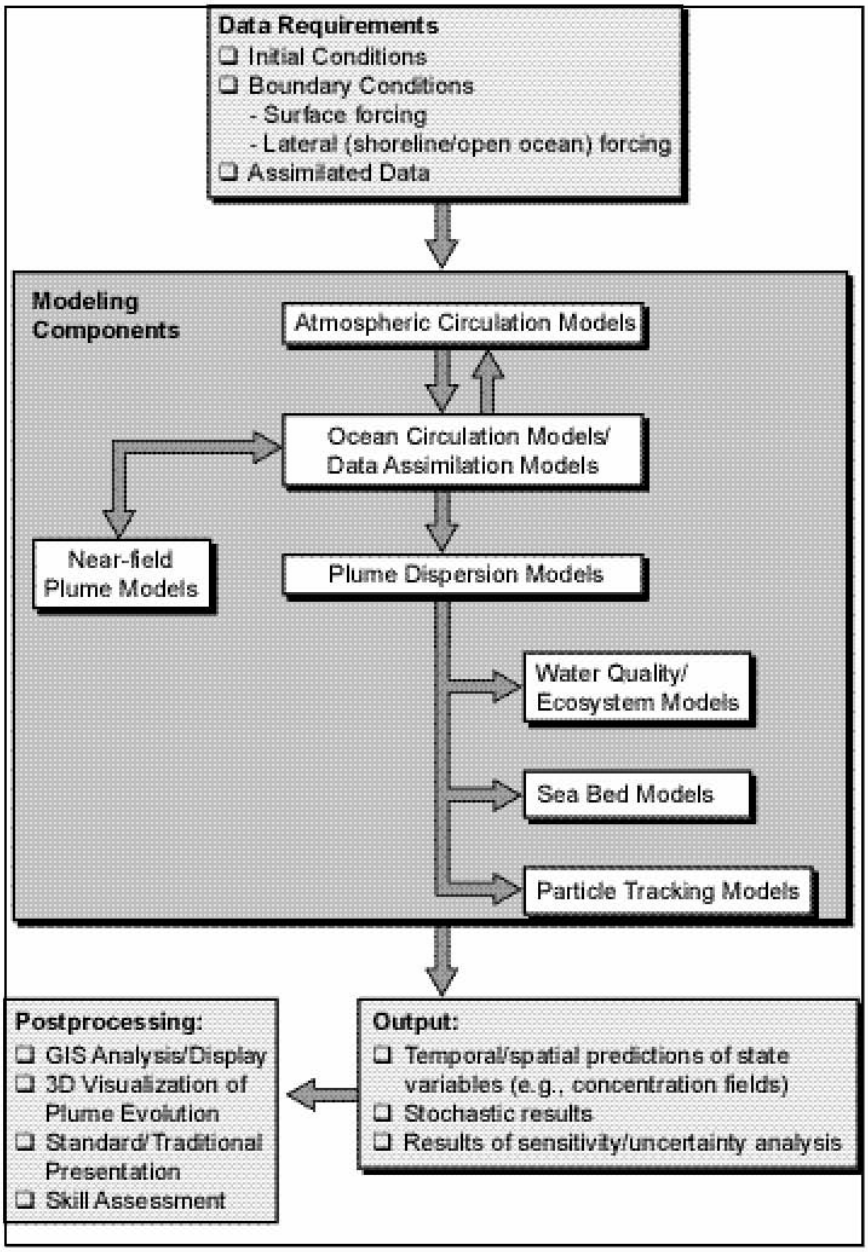

FIGURE 4.1: Circulation and Dispersion modeling components.

The framework depicted is very general, and is intended to be applicable to either diagnostic or prognostic modeling. However, such a framework today probably does not yet exist, at least at the fine temporal and spatial scales needed for circulation and dispersion modeling. Thus the framework in intended to be forward-looking.

The model components box illustrates the range of sub-models that might be needed, depending on the ultimate goal of the investigation. The appearance of an atmospheric circulation model in the figure may be puzzling. In fact, it is expected that an atmospheric circulation model is not needed for present applications. However, in the future, it is likely that atmospheric circulation models will be coupled with circulation models to allow more realistic

exchanges that produce more accurate circulation predictions.

It was shown in Figure 4.1 that the problem of numerical investigation is a complex problem consisting of a number of parts.

The model output can consist of enormously large files of model predictions. These can include time series of predictions at user-specified locations, on snapshots of the spatial distribution of scalars for different times throughout the simulation period. Such output needs to be post-processed so that the results are meaningful. Ultimately, either traditional approaches can be used or newer visualization techniques can be used to display the data three-dimensionally. Visualization techniques are no longer luxuries; they are essential to help understand what the model has predicted. There are a number of models with different scales and grid resolution that is typically simulated, and for which information is generated and data is required. The grid resolutions are specified with the intention to capture the necessary information to make the applications meaningful, but not to be so resolved that the computational time is prohibitive and the problem is never solved. This remains an issue in practically all real-world applications, despite the rapidly increasing speed of computers.

The consideration given above shows that the development of The Specialized Information Analytical Systems (SIAS) is needed to meet the needs of circulation and plume dispersion models. It consists of three subsystems: **Geographic Information System (GIS) and Database Management System (DMS)** and **Analytical Subsystem**. Several mathematical models have been included into the Analytical Subsystem to provide the means for getting dangerous nature parameters for the offshore installations as well as for environment impact estimation. Meteorological models, hydrodynamic models and models of contamination dispersion in the sea environment around offshore installations have been joined into the Hydrodynamic Module named Automation Equipped Working Place (AEWP) “Oceanologist”.

The foregoing models allow the simulation of the meteorological (wind velocity) and hydrodynamic (sea level, current velocity, wind waves) characteristics, which may be dangerous, and the determination of the contamination fields near the offshore installation. The main advantage of the AEWP “Oceanologist” is that the data obtained in one model can be transmitted into the other model as a forcing. The system database serves as an intermediate for data transmission between the models and as a means for data saving. The GIS is needed to visualize the output information on the maps of region.

Common problems that arise while designing information systems are examined from the point of view of joined operation of mathematical models, data bases and Geographic information system, and are presented in Articles [IV], [VI].

REFERENCES

[1] Abramovich G.N. Teorija turbulentnyh struj. Moscow, Fizmatgiz, 1960; Moscow, Nauka, 1984 (in Russian).

[2] Arakawa, A., and Lamb V. R., A potential enstrophy and energy conserving scheme for the shallow water equations. Mon. Wea. Rev ., 109, 1994, pp.18-36.

[3] Arkhipov B.V. About some properties of geophysical hydrodynamic equations on the staggered grid, Journal Oceanology, 29, 5, 1989, pp.723-729.

[4] Arkhipov, BV, Koterov, VN, Solbakov, VV, Model AKS for the Forecast of Dispersion of the Production Disharge from Marine Drilling Platforms, Communication on applied mathematics, Moscow, Computer center of the Russian Academy of Science, 2000.

[5] Astrakhantsev G., Menshutkin V.V., Petrova N.A., Rukhovets L. Modeling of the ecosystems of large lakes, Saint Petersburg, 2003 (in Russian).

[6] Bao-Shi-Shiau, Jia-Jung Juang. Numerical Study on the Far Field Diffusion of Ocean Dumping for Liquid Waste Proc. Eighth Conference ISOPE. Montreal, Vol. 2, 1998, pp.327-334.

[7] Batchelor, G. K., The application of the similarity theory of turbulence to atmospheric diffusion, Q.R. Meteorol. Soc., 76, 1950, pp. 133-146.

[8] Blumberg, A.F., and Mellor G.L., A description of a three-dimensional coastal ocean circulation model. In: Three-Dimensional Coastal Ocean Models, Coastal and Estuarine Science, Vol. 4. (Heaps, N. S., ed.) American Geophysical Union, 1987, pp. 1-19.

[9] Brandsma M.G., Davis L.R., Ayers R.C., Ayers R.C. Jr. *A Computer Model to Predict the Short Term Fate of Drilling Discharges in Marine Environment*. – Proceedings of the Symposium: Research on Environmental Fate and Effects of Drilling Fluids and Cuttings, American Petroleum Institute, Lake Buena Vista, Florida, Jan. 1980

[10] Brandsma M.G., Sauer T.C. *Mud Discharge Model: Report and User's Guide.* Exxon Production Research Co., Houston, Texas, 1983

[11] Bryan, K., A Numerical Method for the Study of the Circulation of the World Ocean, J. Comp. Phys. 4, 1969, p. 347.

[12] Chavent G., Jaffré J., Mathematical Models and Finite Elements for Reservoir Simulation. Studies in Mathematics and its applications. North Holland, Amsterdam, 1986.

[13] Ciarlet P.G., Lions J.L., Handbook of Numerical Analysis, Vol. II, Finite Element Methods, North-Holland, 1991.

[14] Dallemand J.F, Mottram L.C., (ed.) Ecosites, Ecocentres and the implementation of European Union Environment and Sustainable Development Polices, Proceedings of the Final Ecolink Workshop, European Commission, 2004.

[15] Davies A.M., Lawrence J. The response of the Irish Sea to boundary and wind forcing: Results from a three -dimensional hydrodynamic model Journal of geophysical research, 99, C11, 1994, pp. 22,665-22,687.

[16] Dietrich, D. E., and Lin, C. A., Effects of hydrostatic approximation and resolution on the simulation of convective adjustment, Tellus 54(A), 2002, pp. 34-43.

[17] Forsius J, Huttula T. Application of a mathematical model to a branched water course. Geophysica 19:1, 1982, pp. 56-64.

[18] Foxworthy, J. F., R. B. Tibby, and G. M. Barsom, Dispersion of a surface waste field in the sea, Water Pollut. Control Fed., 38, 1966, pp. 1170-1193.

[19] Furukawa K and Wolanski E, Shallow-water frictional effects in island wakes. Estuarine, Coastal and Shelf Science 46, 1998, pp. 599-608.

[20] Gebhart B., Jaluria Y., Mahajan R. I., Sammakia B. Buoyancy-induced flows and transport. Hemisphere Publishing Corporation. Berlin, Heidelberg, New York, London, Paris, Tokyo. 1988.

[21] Gill A. Hydrodynamics of the atmosphere and of the ocean. Moscow, 1986.

[22] Grammeltvedt, A., A survey of finite-difference schemes for the primitive equation for a barotropic fluid. Mon. Wea. Rev., 97, 1969, pp. 384–404.

[23] Huttula T. (ed.), System analysis applications to water research in the Sovjet Union and Finland. Publications of Water and Environment Institute No. 3, National Board of Waters and Environment, Helsinki, 1989.

[24] Kardestuncer H., Norrie D. H., (ed.) Finite Element Handbook, New York, 1987.

[25] Kochin N.E. Kibel I.A. Rose N.V. Theoretical hydromechanics. Moscow, Gos. Izdat. Fizico-Matematichescoy Literatury, 1963.

[26] Koh R.C.Y., Brooks N.H. Fluid Mechanics of Wastewater disposal in ocean – Annual Review of Fluid Mechanics, 7, 1975, pp. 187-211.

[27] Koh R.C.Y., Chang Y.C. Mathematical Model for Barged Ocean Disposal of waste, U.S. EPA, Technical Report 660/2-73-029, Washington, D.C., 1973.

[28] Kolmogorov, A.N., Local Structure of a Turbulence in an Incompressible Liquid at Very Major Reynolds Numbers, DAS of the USSR, 30, 4, 1941, pp. 299-306.

[29] Koponen, J., Alasaarela, E., Lehtinen, K., Sarkkula, J., Simbierowicz, P., Vepsä, H., Virtanen, M. , Modelling the Dynamics of a Large Sea Area, Publications of the Water and Environment Research Institute No 7, National Board of Waters and the Environment, Finland, Helsinki, 1992.

[30] Kulikovskii A.G., Pogorelov N. V and Semenov A.Yu. Mathematical Problem of Numerical Solution of Hyperbolic Systems. Moscow, 'Fizmatlit' Publishing House, 2001 (in Russian).

[31] Lebedev V. V. and Turitsyn K. S., Passive scalar evolution in peripheral regions, Physical review, 69, 2004, pp. 036301.1 - 036301.11.

[32] Lloyd PM, Stansby PK, Shallow-water flow around model conical islands of small side slope. 1: Surface piercing. Journal of Hydraulic Engineering, 123, 1997, pp. 1057-1067.

[33] Luyten P.J., Deleersnijder E., Ozer J., Ruddick K.G. Presentation of a family of turbulence closure models for stratified shallow water flows and preliminary applications to the Rhine outflow region, Continental Shelf Research, 16. 1, 1996, pp.101-130.

[34] Marchuk G.I. Methods of Numerical Mathematics, 2nd edn., Springer, Verlag, New York, Berlin, 1982.

[35] Mellor G.L., Yamada T., Development of a turbulence closure model for geophysical fluid problems, Rev. Geophys., 20, 1982, pp. 851–875.

[36] Monin, A.S., and Ozmidov R.V., Turbulence in the Ocean, D. Reidel, Norwell, Mass., 1985.

[37] Monin, AS, Yaglom, AM, Statistical Hydromechanics, Part 2, Moscow, 1967.

[38] Murthy, C. R., Horizontal diffusion characteristics in Lake Ontario, /. Phys. Oceanogr., 6, 1976, pp. 76-84.

[39] Obuhov, AM, About an Energy Distribution in a Spectrum of a Turbulent Current, Izv. AN of the USSR, Geographic and geophysics series. B. 5, 4-5, 1941, pp. 453-462.

[40] Okubo, A., Oceanic diffusion diagrams, Deep-Sea Research, 18, 1971, pp. 789-802.

[41] Oliger, J. and Sundstreom, A., Theoretical and practical aspects of some initial boundary value problems in fluid dynamics, SIAM J. Appl. Math 35, 1978, pp. 419–446.

[42] Orlanski, I., A simple boundary condition for unbounded hyperbolic flows, J. Comp. Phys. 21, 1976, pp. 251–269.

[43] Ozmidov, RV, Diffusion of Contaminants in Ocean, Leningrad, Gidrometeoizdat, 1986.

[44] Palma, E. D. and Matano, R. P. On the implementation of open boundary condition for a general circulation model: The three-dimensional case. J. Geophys. Res., 105, 2000, pp. 8605-8627.

[45] Pearson Karl, The Problem of the Random Walk, Nature, LXXII, 1905, pp. 72-294.

[46] Pearson, R., Consistent boundary conditions for numerical models of systems that admit dispersive waves, J. Atmos. Sci., 31, 1974, pp 1481–1489.

[47] Peeters F., Wuest A., Piepke G., and Imboden D. M., Horizontal mixing in lakes, Journal of Geophysical Research, 101, C8, 1996, pp. 18,361-18,375.

[48] Podsetchine V., Huttula T. Numerical simulation of wind-driven circulation in Lake Tanganika. Aquatic Ecosystem Health and Management: Tampere, Finland, 3, 1, 2000, pp. 55-64.

[49] Prandl L. Hydromechanics. Moscow, Izdatelstvo Inostrannoy Literatury, 1949.

[50] Richardson L.F. Atmospheric diffusion shown on a distance-neighbor graph Proc. Roy. Soc. Ser. A., 110, 756, 1926, pp. 709-720.

[51] Roed L.P., Cooper C. Open boundary conditions in numerical ocean models, in Advanced Physical Oceanographic Numerical Modeling, edited by J.J. O'Braien, NATO ASI Ser. C, 186, 1986, pp. 411-436.

[52] Sarkkula J., Virtanen M., Modeling of water exchange in an estuary. Nordic Hydrology, 9, 1978, pp. 43-56.

[53] Sarkkula, J. Measuring and Modeling Flow and Water Quality in Finland. VITUKI Monographies 49, Water Research Center VITUKI, Budapest, 1989.

[54] Schernewski, G., Podsetchine V., Asshoff M., Garbe-Schönberg D., Huttula T., Spatial ecological structures in littoral zones and small lakes: Examples and future prospects of flow models as research tools. Archiv für Hydrobiologie, Advances in Limnology, 55, 2000, pp. 227-241.

[55] Schernewski, G., V. Podsetchine, H. Siegel and T. Huttula, Instruments for water quality management and research in coastal zones: Flow and transport simulations across spatial scales Periodicum biologorum, 102, 1, 2000, pp. 65-75.

[56] Tseng Yu-Heng, Ferziger Joel H., A ghost-cell immersed boundary method for flow in complex geometry, Journal of Computational Physics, 192, 2003, pp. 593 - 623.

[57] Uusitalo S., The Numerical Calculation of Wind Effect on Sea Level Elevations, Tellus, 12, 4, 1960, pp. 427-435.

[58] Virta H., 3D model of Lake Pääjärvi. MSc. Thesis at the Department of Geophysics. University of Helsinki, 2001.

[59] Ward, G. H., Jr., Dye diffusion experience in the Texas bays: Low-wave conditions, Geophys. Res., 90, 1985, pp. 4959-4968.

[60] Wuest A, Piepke G, Van Senden DC, Turbulent kinetic energy balance as a tool for estimating vertical diffusivity in wind-forced stratified waters. Limnol. Oceanogr., 45, 2000, pp. 1388–400.